

# IR11688 SmartRectifier™ Control IC Design Notes

Authors: Helen Ding  
Peter Green

Application Note

## About this document

### Scope and purpose

The purpose of this document is to provide a comprehensive functional description and guide to using the IR11688 dual channel synchronous rectification control IC in the output of a LLC switch mode power supply (SMPS). The scope applies to all technical aspects that should be considered in the design process, including calculation of external component values, MOSFET selection, PCB layout optimization as well as additional circuitry that may be added if needed in certain cases.

### Intended audience

Power supply design engineers, applications engineers, students.

## Table of Contents

<b>1</b>	<b>Introduction and device overview.....</b>	<b>3</b>
<b>2</b>	<b>SmartRectifier™ concept and IR11688 operation.....</b>	<b>4</b>
<b>3</b>	<b>Design and selection of passive components .....</b>	<b>7</b>
3.1	IR11688 V <sub>CC</sub> supply.....	7
3.2	MOT resistor calculation .....	8
3.3	Gate driver resistor.....	8
3.4	Gate resistor and IC power loss calculation .....	8
<b>4</b>	<b>Other application information .....</b>	<b>11</b>
4.1	MOT protection .....	11
4.2	Turn-on blanking time and VD filter .....	12
4.3	Early turn-off and regulation phase .....	13
4.4	Light load ripple .....	15
4.5	Gate clamping circuit for logic level MOSFET .....	18
<b>5</b>	<b>SR MOSFET power loss calculation and MOSFET selection.....</b>	<b>19</b>
5.1	Body diode conduction loss at turn-on.....	19



---

**Introduction and device overview**

5.2	Conduction loss in regulation phase.....	20
5.3	Channel conduction loss.....	20
5.4	Body diode conduction loss at turn-off.....	21
5.5	Switching loss.....	21
5.6	Gate charge loss .....	25
5.7	MOSFET selection guide.....	25
6	<b>PCB layout guidelines and examples .....</b>	<b>26</b>
7	<b>Appendix: Transformer leakage inductance and modeling.....</b>	<b>28</b>
8	<b>Appendix: Symbols list.....</b>	<b>33</b>

# 1 Introduction and device overview

The IR11688 synchronous rectifier (SR) control IC drives a pair of N-channel power MOSFETs forming the rectifying output stage of a resonant half-bridge converter. The drain to source voltage of each SR MOSFET is directly sensed to determine the level of conducted current so that the MOSFET can be turned on and off in close proximity to the zero current transition. Built in shoot-through protection logic prevents both channels from being able to ever turn on at the same time. Internal blanking, reverse current protection and double-pulse suppression allow reliable operation in all operating modes.

The IR11688 precisely controls switching on and off of the synchronous MOSFETs thereby bypassing their body diodes during the secondary conduction phases and emulating the rectifying action of a dual diode rectifier while eliminating the majority of conduction losses. The MOSFET drain to source voltages are sensed at millivolt levels to determine the magnitude and polarity of the drain current so that the IR11688 can switch the gates on and off appropriately. The high voltage input structure allows the IR11688 to withstand up to 200 V from direct connection to each drain pin.

The IR11688 based smart synchronous rectifier offers significant efficiency improvement in resonant converters over the full load range. Replacement of a Schottky diode output rectifier with the IR11688 combined with a pair of correctly selected high performance MOSFETs, provides significantly lower power dissipation and efficiency improvement. PCB space savings due to the IR11688's small SO-8 package are further aided by reduced MOSFET heat dissipation.

The IR11688 can operate from a wide Vcc supply voltage ranging from 4.75 V to 20 V enabling it to be supplied from the output in a 5 V system and eliminating the need for an auxiliary transformer winding. A logic level MOSFET is required for low output (low Vcc) voltage applications.

A built in arming and triggering mechanism allows correct switching on and off of the SR MOSFET under all system conditions, making it superior to a basic self-driven SR scheme or earlier generations of SR controller.

In addition the IR11688 enters a power saving mode if both VD sensing inputs do not switch for more than a waiting time (typically 500 μs). Supply current reduces to a few hundreds of micro-Amps, greatly reducing quiescent power loss in standby mode and improving system standby and light load efficiency.

IR11688 is available in a SO-8 package. The pin out is shown below:

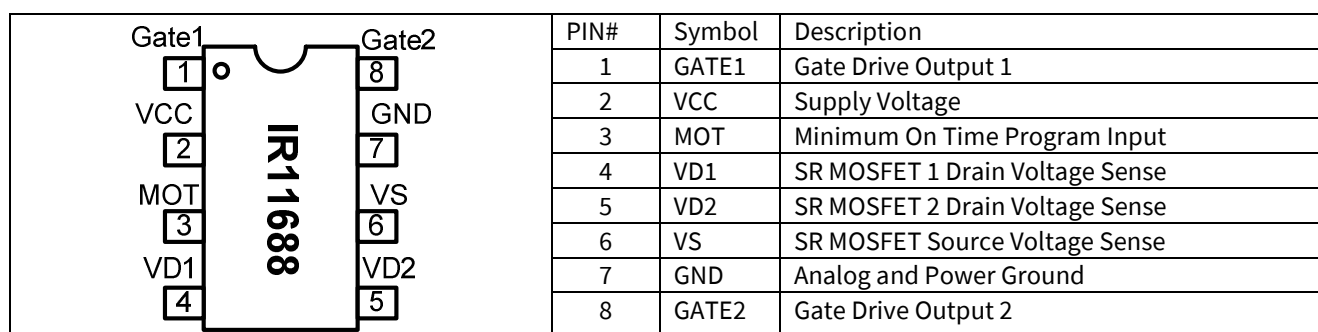


Figure 1 IR11688 Dual SmartRectifier™ control IC pin assignment



SmartRectifier™ concept and IR11688 operation

delivered to load through the output rectifier circuit. At this point the conduction phase of the branch SR MOSFET is initiated and current starts flowing through its body diode, producing a negative  $V_{DS}$  voltage. The body diode has a much higher voltage drop than the turn-on threshold  $V_{TH2}$  causing the IR11688 to drive the gate of the SR MOSFET on to bypass it.

When the MOSFET is turned on the instantaneous sensed voltage reduces to  $R_{DSon} \cdot I_D$ . This voltage level being much lower than body diode forward voltage drop is sensitive to parasitic ringing generated by the transformer leakage inductance and MOSFET output capacitance. To avoid mis-triggering and resulting premature gate turn-off, a blanking period (MOT) is set that disables  $V_{TH1}$  triggering for a minimum period of time set by an external resistor. This avoids false triggering of the turn-off immediately after turning-on, by maintaining the MOSFET on for a minimum amount of time.

Once the SR MOSFET has been turned on, it will remain on until the rectified current decays to a level where  $V_{DS}$  reaches the regulation threshold  $V_{THR}$ . At this point the gate drive pull up is switched off and the gate drive output remains in a high impedance state with a weak pull down to slowly discharge the gate voltage. The MOSFET channel resistance increases as gate voltage drops moving towards the linear region of operation and thereby maintaining the negative  $V_{DS}$  voltage drop lower than the turn off threshold  $V_{TH1}$ . The discharge circuit is maintained to keep  $V_{DS}$  voltage regulated around  $V_{THR}$  as current falls, thereby extending the MOSFET conduction period.

Eventually as the MOSFET channel current reduces further towards zero, the  $V_{DS}$  voltage crosses threshold  $V_{TH1}$  and the IR11688 turns the gate off. The gate drive regulation function is illustrated in figure 4:

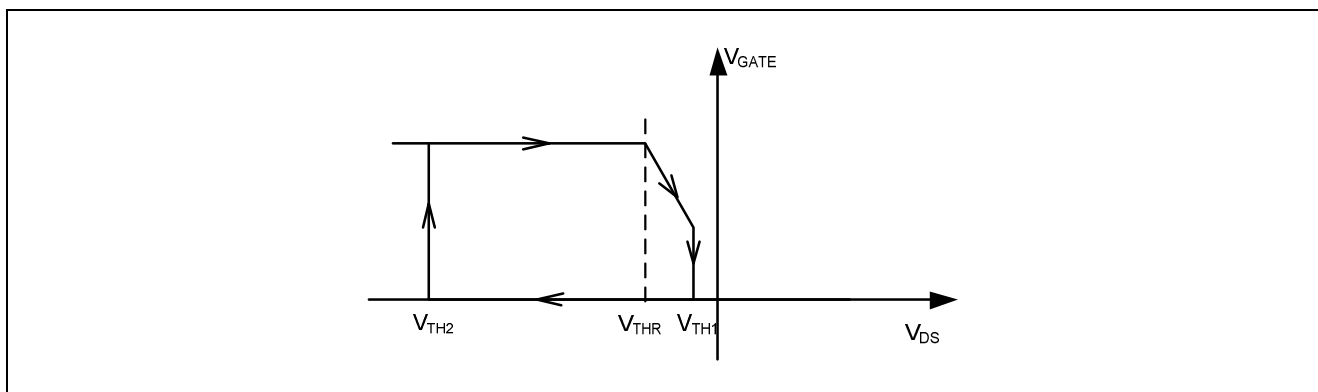


Figure 4 IR11688 voltage sensing thresholds

When the IR11688 turns the gate off current will again start flowing through the body diode, which causes the  $V_{DS}$  voltage to make a sharp negative transition. Depending on the amount of residual current,  $V_{DS}$  may once again exceed the turn on threshold  $V_{TH2}$ . For this reason re-triggering is disabled after the gate drive has been switched off until the controller has re-armed.

The re-arming sequence requires  $V_{DS}$  to cross the  $V_{TH3}$  threshold and remain above it for a period denoted as  $t_{BRST}$ . If this does not occur the gate drive will remain low for a period of  $t_{BLANK}$ , after which time re-arming will occur automatically.

To achieve high system efficiency combined with low standby loss, the IR11688 incorporates a programmable minimum on time (MOT). This feature offers flexibility when using the IR11688 in various applications operating at different switching frequencies. The MOT function effectively sets the shut-down point at light load. During normal operation, the designer sets the minimum on time to be shorter than the secondary conduction period. At progressively lighter loads, the conduction period reduces until it is eventually shorter than the MOT. If the IR11688 detects no voltage drop signifying no SR drain current the MOT protection function causes the gate drive to be disabled for the next cycle. This MOT protection operates whether or not the SR gate drive is on, that is if conduction is through drain-source channel or the

SmartRectifier™ concept and IR11688 operation

body diode. In this way the IR11688 does not drive the gate at light loads and therefore consumes minimal power improving system efficiency.

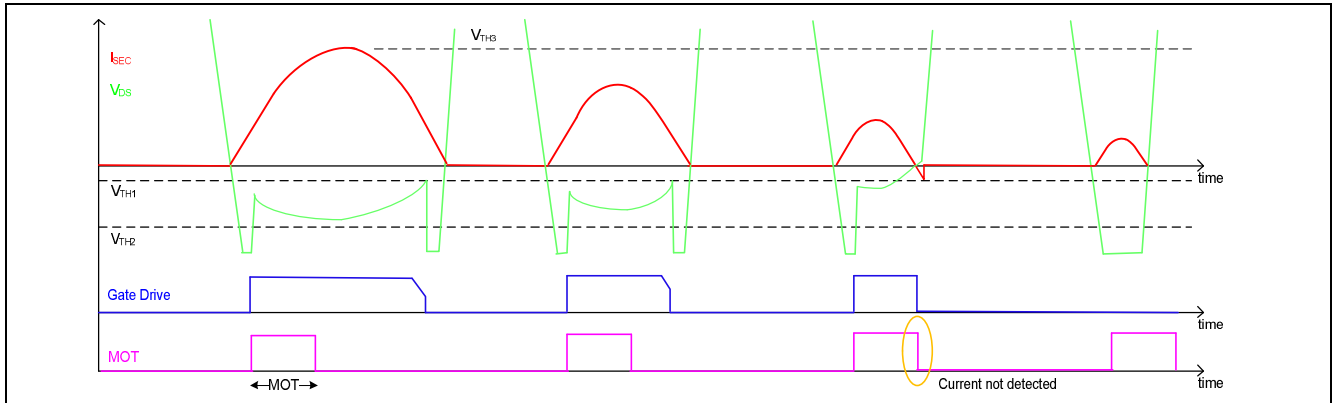


Figure 5 MOT protection as load decreases

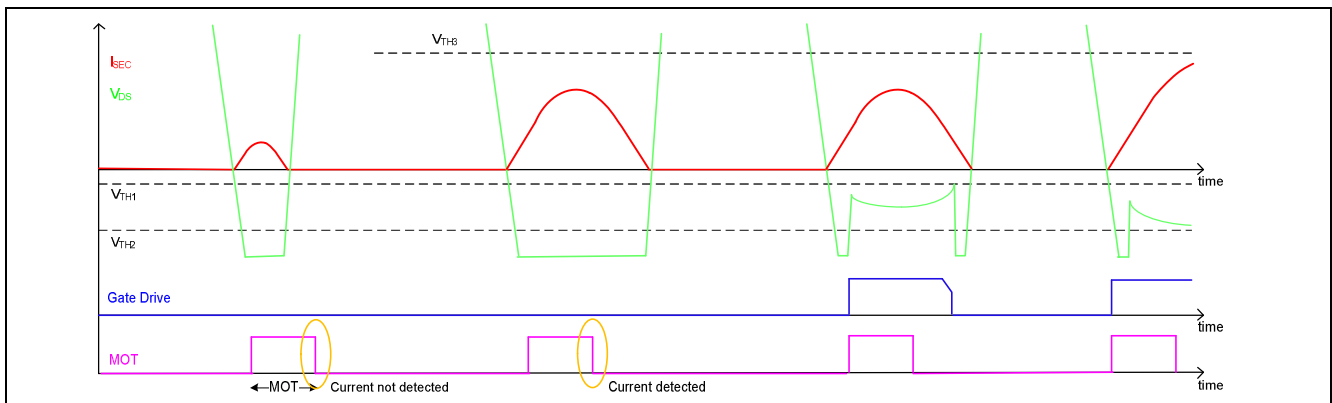


Figure 6 Gate drive resuming as load increases

The IR11688 includes a turn-on leading edge blanking function to prevent misfiring that could be triggered by high frequency ringing in DCM operation. In DCM mode the drain voltage of the SR MOSFET can resonate when secondary current transitions in each half cycle. This  $V_{DS}$  ringing as shown in figure 3 could drop below zero volts under certain conditions, such as higher body diode voltage drop or longer body diode reverse recovery. To avoid false triggering by negative ringing, the IR11688 only triggers if  $V_{DS}$  is lower than  $V_{TH2}$  longer than blanking time  $T_{bon}$ . Therefore, in the case of a short spike or ringing the IR11688 will not switch on the MOSFET gate and the internal MOT timer will not be initiated preventing a false trigger event and resulting shoot through current. In a regular conduction cycle  $V_{DS}$  remains lower than  $V_{TH2}$  for more than  $T_{bon}$ , and so the gate turns on after  $T_{bon}$  expires.

The total turn on delay  $T_{don}$  is the sum of  $T_{bon}$  blanking time and the propagation delay of internal comparator. The turn-on delay  $T_{don}$  and the MOT time limit the minimum conduction time of the secondary rectifiers and hence, the maximum switching frequency of the converter with which it can effectively operate.



## Design and selection of passive components

$0.5 + V_{CCON}$  before the IR11688 gate drives are enabled (the voltage drop through  $R_{VCC}$  is negligible since  $R_{VCC} \leq 10 \Omega$ ). This prevents possible shoot through from occurring due to the gates potentially being switched on due to ringing oscillations during start up.

### 3.2 MOT resistor calculation

The MOT is linear in relation to the resistor value  $R_{MOT}$ , the following formula can be used to determine the required value:

$$R_{MOT} = 5 \cdot 10^{10} t_{MOT} \quad (1)$$

The value of  $R_{MOT}$  should not be lower than the minimum recommended on the datasheet.

### 3.3 Gate driver resistor

Since IR11688 based synchronous rectification turns the SR MOSFETs on and off at  $V_{DS}$  levels close to zero, the gate resistors do not have an impact on the transitions and can be designed in order for the gate loop to be optimized and oscillations should be minimized as much as possible in regular operations. Therefore, assuming the total gate trace loop inductance ( $L_g$ ) is known, (a first order estimation can be 1 nH/mm of physical trace length), the minimum recommended gate resistor will be:

$$R_{g_{loop}} > 2 \sqrt{\frac{L_g}{C_{iss}}} \quad (2)$$

where  $C_{iss}$  is the input capacitance from the MOSFET datasheet. It is evident how a correctly optimized layout can dramatically reduce the gate resistance requirement.

$R_{g_{loop}}$  is the total resistance in the gate charge loop:

$$R_{g_{loop}} = R_{down} + R_{g_{FET}} + R_g \quad (3)$$

$R_{down}$  is the internal pull down resistance of the IR11688 gate drivers;  $R_{g_{FET}}$  is the internal gate resistance of the SR MOSFET and  $R_g$  is the external gate resistor. Typical values of  $R_{down}$  and  $R_{g_{FET}}$  are good enough for this calculation.

Rearranging the equation gives:

$$R_g = R_{g_{loop}} - R_{g_{FET}} - R_{down} \quad (4)$$

### 3.4 Gate resistor and IC power loss calculation

To calculate IR11688 current consumption the gate charge of the synchronous MOSFETs needs to be determined. The secondary current initially flows through the body diode of each SR MOSFET, which will therefore be turned on in ZVS mode. In zero-voltage switching operation the MOSFET behaves like a constant capacitance load ( $C_{sync}$ ) connected to the IC gate drive output because the variation of  $C_{sync}$  with  $V_{GS}$  is negligible.

The following diagram shows how the normal gate characteristics (Magenta) change when the switch is turned on at zero voltage (Blue). The gate plateau is effectively eliminated:

Design and selection of passive components

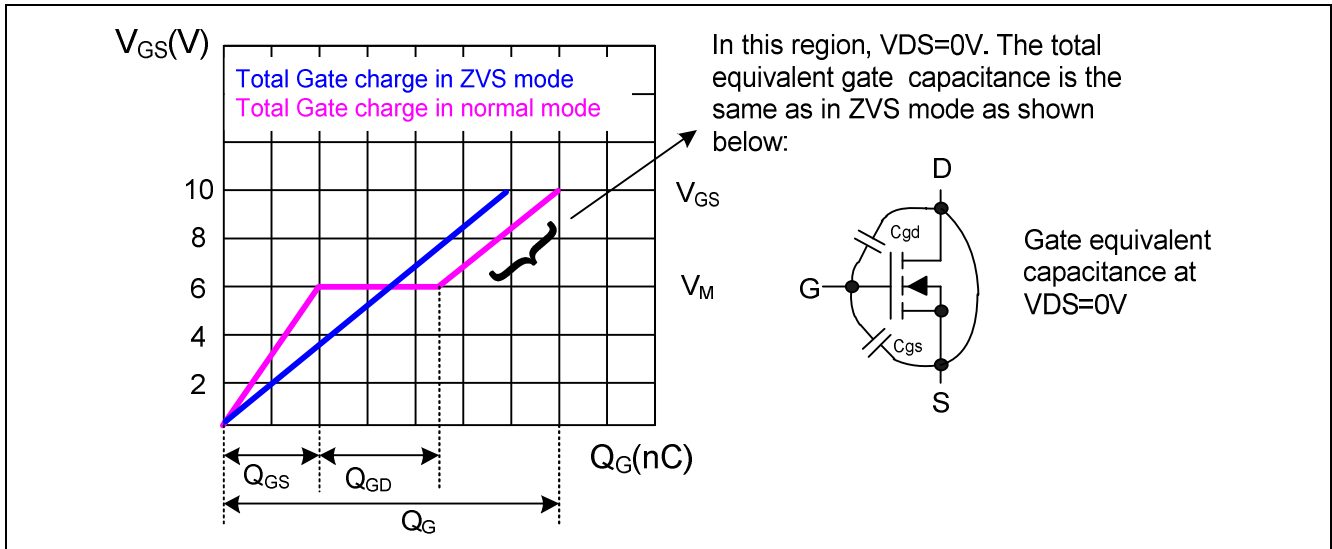


Figure 9 MOSFET gate equivalent capacitance in ZVS mode

$$C_{sync} = \frac{(Q_g - Q_{gd} - Q_{gs})}{V_{gs} - V_m} \tag{5}$$

$V_{gs}$  is the gate voltage where  $Q_g$ ,  $Q_{gd}$  and  $Q_{gs}$  are tested. In most datasheets it is specified as 10 V.  $V_m$  is the Miller plateau voltage. If two or more MOSFETs are connected in parallel, the above capacitance is multiplied by the number of devices.

The IC operating current can be calculated from the following equation:

$$I_{CC} = I_{QCC} + 2 \cdot f_{SW} C_{sync} V_{cc} + (0.285 \cdot V_{cc} - 0.425) \cdot 10^{-9} f_{SW} \tag{6}$$

where  $f_{SW}$  is the converter switching frequency. The first term is the quiescent current of the IR11688 in active mode. The second term is gate driver loss due to the synchronous MOSFET equivalent capacitance, while the third term accounts for the IC internal logic consumption during regular operation (the frequency dependent current requirements for the internal logic).

Not all the gate driver losses are dissipated in the IR11688. Losses are actually shared between the IC package, the external gate resistor and the MOSFET gate resistor. These resistances are in series in the gate driver loop, which means they will proportionally share the power dissipation.

The total power dissipated by the driver and the total gate resistance is calculated as follows. Calculations are based on a single channel.

$$P_{dr} = C_{sync} \cdot V_{cc}^2 \cdot f_{SW_{max}} \tag{7}$$

The driver buffer and the gate resistance will linearly share this power dissipation as described in the following relationship:

$$P_{R_{g_{ext}}} = \left( \frac{R_g + R_{gFET}}{R_g + R_{gFET} + R_{Source}} + \frac{R_g + R_{gFET}}{R_g + R_{gFET} + R_{Sink}} \right) \cdot \frac{P_{dr}}{2} \tag{8}$$

Solving this equation with respect to  $R_{g_{ext}}$  (which includes the external gate resistor  $R_g$  and the MOSFET internal gate resistance  $R_{gFET}$ ), it is possible to determine the percentage of the total driving power dissipated in the gate resistor as a function of its value. Notice that in the IR11688 datasheet, pull up ( $r_{up}$ )

---

## Design and selection of passive components

and pull down ( $r_{down}$ ) resistances are defined. For the above calculations, we use  $R_{Sink} = 2r_{down}$  and  $R_{Source} = 2r_{up}$  in order to allow for temperature drift and process variation.

The power loss in the IR11688 can now be calculated as:

$$P_{IC} = V_{cc} \cdot I_{cc} - 2 \cdot P_{R_{g_{ext}}} \quad (9)$$

It is clear that reducing supply voltage  $V_{cc}$  or increasing external gate resistor could effectively reduce SR controller IC power dissipation.

## 4 Other application information

### 4.1 MOT protection

At very light load or no load conditions, the secondary branch conduction period is likely to be less than the MOT period. If the SR is triggered then the MOSFET current will flow backwards from drain to source towards the end of the MOT period. This reverse current discharges the output capacitor causing energy to be transferred back to the transformer. Leakage inductance resonates with circuit capacitances resulting in ringing oscillations appearing at  $V_{DS}$  after the SR MOSFET turns off. This ringing can potentially cause the SR controller to mis-trigger and turn on the gate, creating more reverse current and subsequent multiple false triggering events as illustrated below:

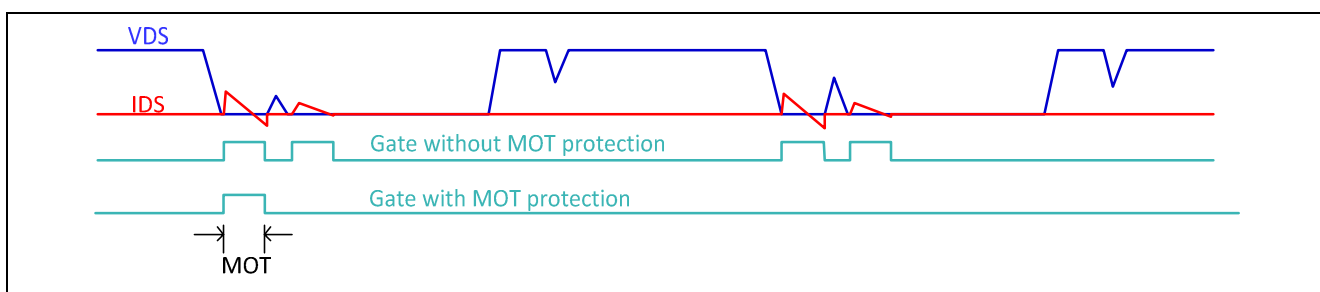


**Figure 10** MOT protection waveform

The cycle-by-cycle MOT protection circuit of the IR11688 detects this reverse current condition and disables the following gate output pulse. This protection operates whether or not the gate drive is turned on so that a single event disables the SR until conduction has again been detected at the end of the MOT period. The pale blue waveforms in figure 10 compare SR gate drive behavior with and without MOT protection. The IR11688 continuously monitors load current and returns to normal operating mode once it has increased so that the conduction time is longer than the MOT.

Unlike the earlier IR11682, the IR11688 MOT duration is externally programmable via a resistor ( $R_{MOT}$ ) so that the user may set the trigger threshold at a desired load point below which the gate of IR11688 will be disabled by MOT protection. This function helps to reduce standby power losses.

Figure 11 shows a typical MOT cycle skipping waveform in an IR11688 based synchronous rectifier operating at light load. In this example the current conduction time in the SR is longer than the MOT. However since the output current is very low, the  $V_{DS}$  voltage drop of the MOSFET is already less than  $V_{TH1}$  at the end of MOT and consequently the IR11688 skips the next cycle. The body diode forward voltage drop during this next cycle is then sufficient to re-enable the gate output for the subsequent cycle. Under this borderline load condition, the IR11688 enables gate output every alternate cycle where the gate pulse width of each cycle is equal to the MOT. This operation is normal with the IR11688 and should not be cause for concern.

The IR11688 has independent MOT protection for each channel. It is therefore possible to for one channel to have MOT cycle skipping and the other channel to display normal operation, if channel 1 and channel 2 currents are not perfectly balanced.

Other application information

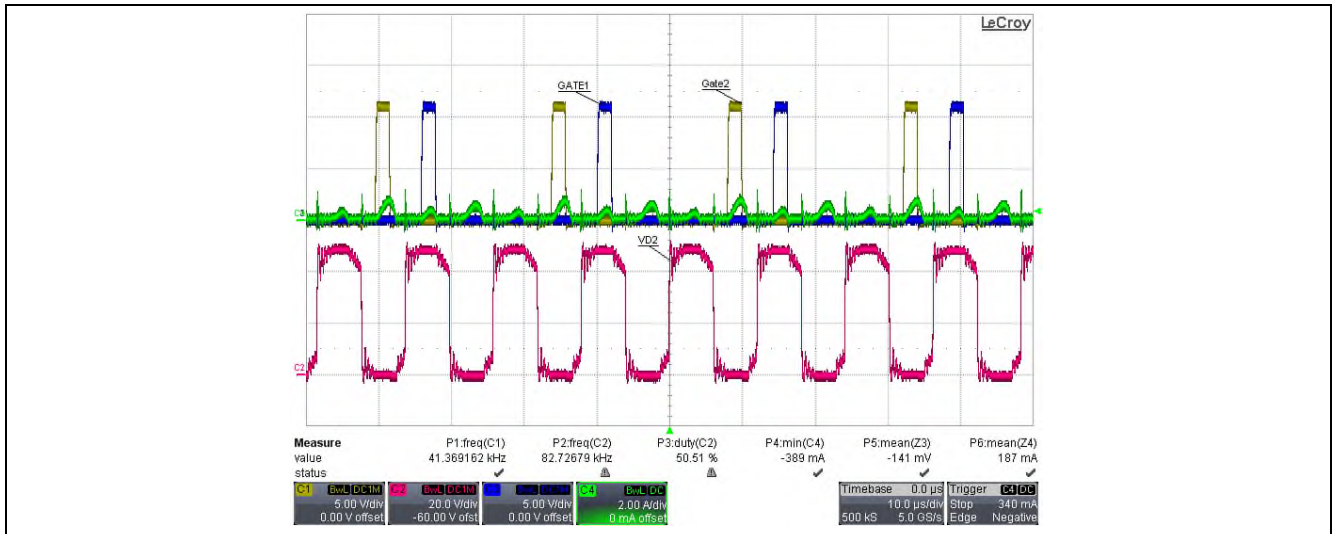


Figure 11 Waveform at light load with MOT pulse skipping

### 4.2 Turn-on blanking time and VD filter

As explained previously, the IR11688 incorporates leading edge blanking time and is therefore capable of preventing false triggering caused by ringing. The oscilloscope traces below show how the negative ringing is blanked so that the IR11688 only turns on the gate drive during the normal conduction period.

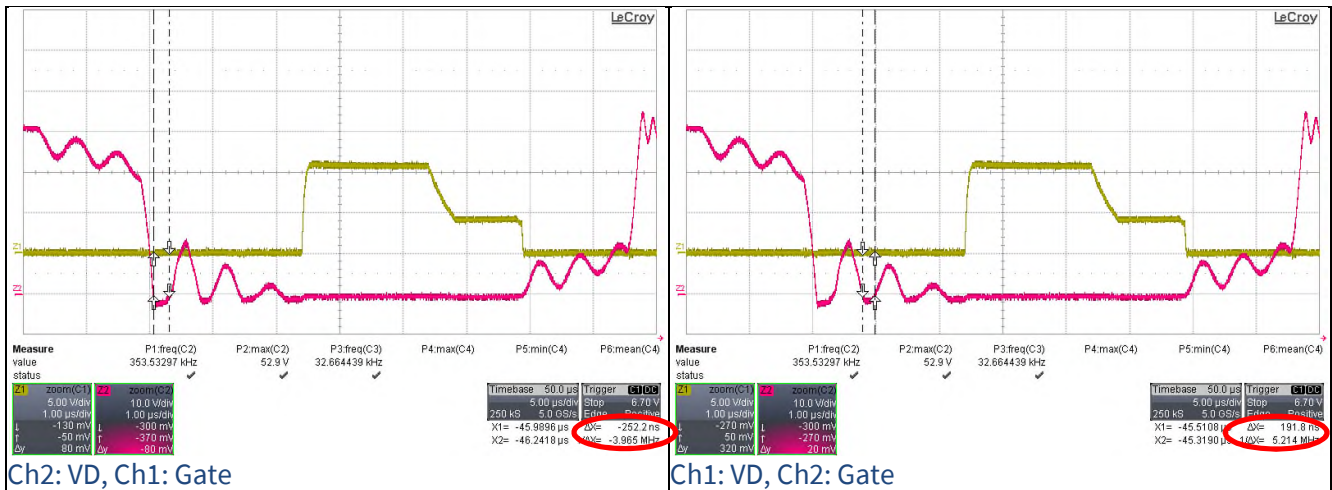


Figure 12  $V_D$ s ringing at the beginning and the end of a switching cycle

The leading edge blanking time of the IR11688 is internally fixed. In cases where a longer filtering time is desired, a small additional RC delay may be added at the  $V_D$  input. To avoid bias current offsetting the  $V_D$  sensing voltage on the external resistor, the value of this resistor should not be higher than 1 k $\Omega$ .

Other application information

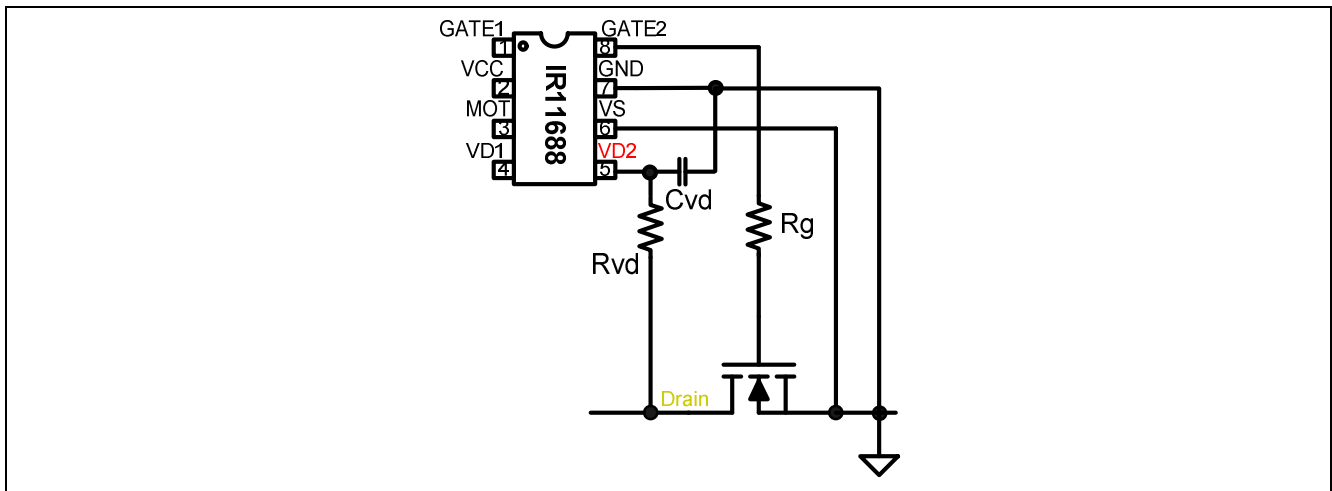


Figure 13 RC filter of VD pin

As shown in Figure 14, ringing with a 311 ns negative pulse width is filtered by a 1 kΩ + 47 pF RC network connected from the drain to the V<sub>D</sub> pin greatly reducing the negative peak to prevent false triggering.

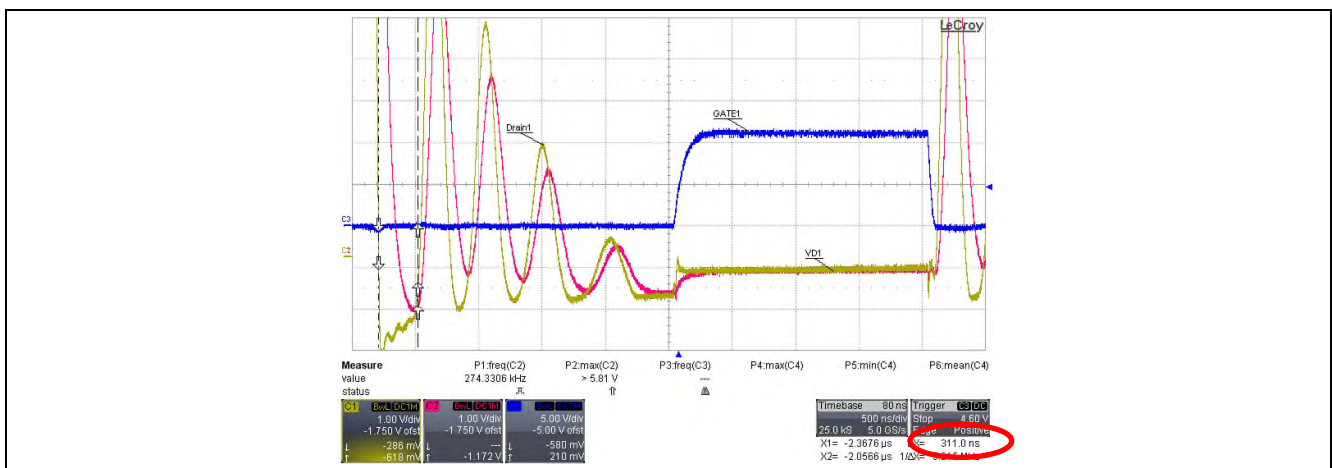


Figure 14 V<sub>D</sub> waveform with 1 kΩ 47 pF filter (C1: Drain of SR MOSFET, C2: V<sub>D</sub> waveform after RC filter, C3: Gate)

### 4.3 Early turn-off and regulation phase

As illustrated here, the parasitic inductance in series with the SR MOSFET tends to create a voltage drop resulting from the falling current. This would degrade the effectiveness of the SR controller voltage-sensing control technique by cancelling out drain to source voltage drop so that the SR controller switches off gate drive prematurely. Though the designer should always optimize the PCB layout as far as possible to minimize stray inductance, obtaining a true Kelvin contact to the MOSFET depends on the device package, die bonding and lead lengths. Through-hole packages such as TO-220 and TO-247 generally have larger stray inductances than surface mount packages like QFN, SO-8, or DirectFET. Even a small amount of inductance combined with a typical current slew rate can cause a voltage drop in the range of the IC’s milli-volt switch off threshold levels ( $V_{TH1}$ ). The effect is to trigger IC turn-off gate before drain current has fallen to  $V_{TH1}/R_{DSon}$  as in the ideal case.

Other application information

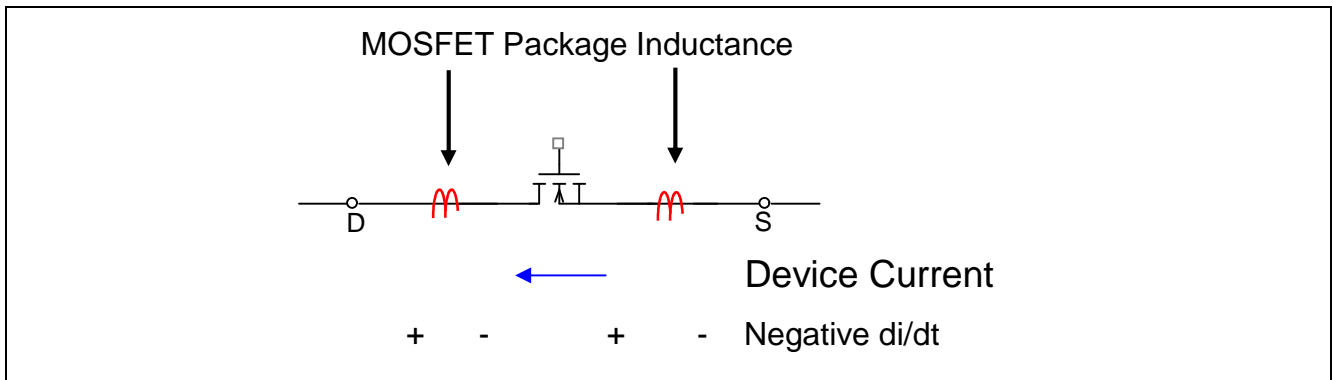


Figure 15 MOSFET package inductance

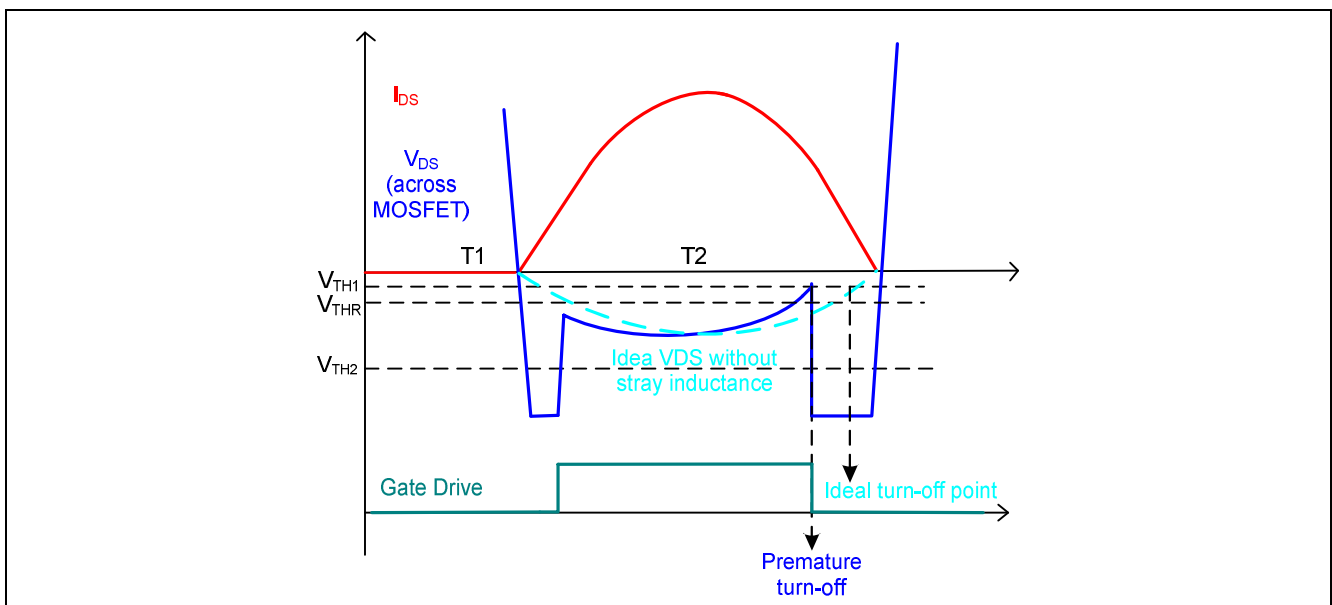


Figure 16 Premature turn-off waveform

Premature gate turn-off creates increased body diode conduction loss in the SR MOSFET since it is conducting through the body diode over a longer period. To overcome this problem, the IR11688 incorporates a gate voltage regulation function. In this way the SR MOSFET gate is pulled high only during the MOT period and after this the internal gate pull up is turned off so that the gate output enters a high impedance tri-state mode as previously mentioned. The gate voltage remains high due to the charge held by SR MOSFET equivalent gate capacitance. When the  $V_{DS}$  voltage increases to -40 mV, an internal slow discharge circuit is activated to gradually discharge the gate voltage. As a result the channel resistance of the SR MOSFET increases as the gate voltage decreases. The IR11688 stops discharging the gate voltage when  $V_{DS}$  falls below -50 mV. In this way  $V_{DS}$  is regulated between -40 mV and -50 mV. This function helps to compensate premature turn-off by maintaining a voltage at  $V_D$  above the  $V_{TH1}$  switch off threshold down to very low current levels. This minimizes body diode conduction time at switch off and compensates for the effects of parasitic inductance.

Other application information

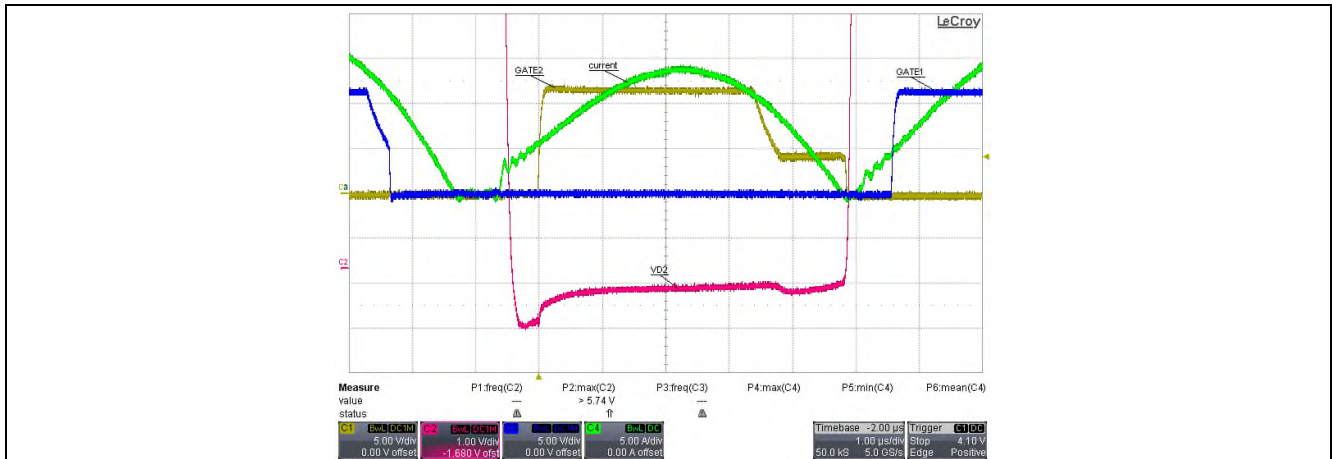


Figure 17 IR11688 regulation phase at turn-off

A MOSFET with a smaller  $Q_g$  will work more effectively with the IR11688. This is because a MOSFET with large  $Q_g$  may not be able to utilize the regulation function and may therefore still have premature turn-off under a high  $di/dt$  condition. Figure 18 shows the gate 1 waveform, (blue trace) is discharged to 5.5 V in the regulation phase. Since MOSFET drain to source resistance does not change linearly with gate voltage, the channel resistance is not increased enough at 5.5 V  $V_{gate}$  to compensate the voltage offset created by stray inductance. Gate 1 is turned off when  $V_{DS}$  voltage reaches  $V_{TH1}$ . At this point MOSFET current is 4 A therefore significant body diode conduction loss occurs.

Reducing the  $V_{CC}$  supply voltage can improve the performance of the IR11688 when driving large MOSFET, since the initial gate drive voltage is limited to  $V_{CC}$ .

This is illustrated in following waveforms:

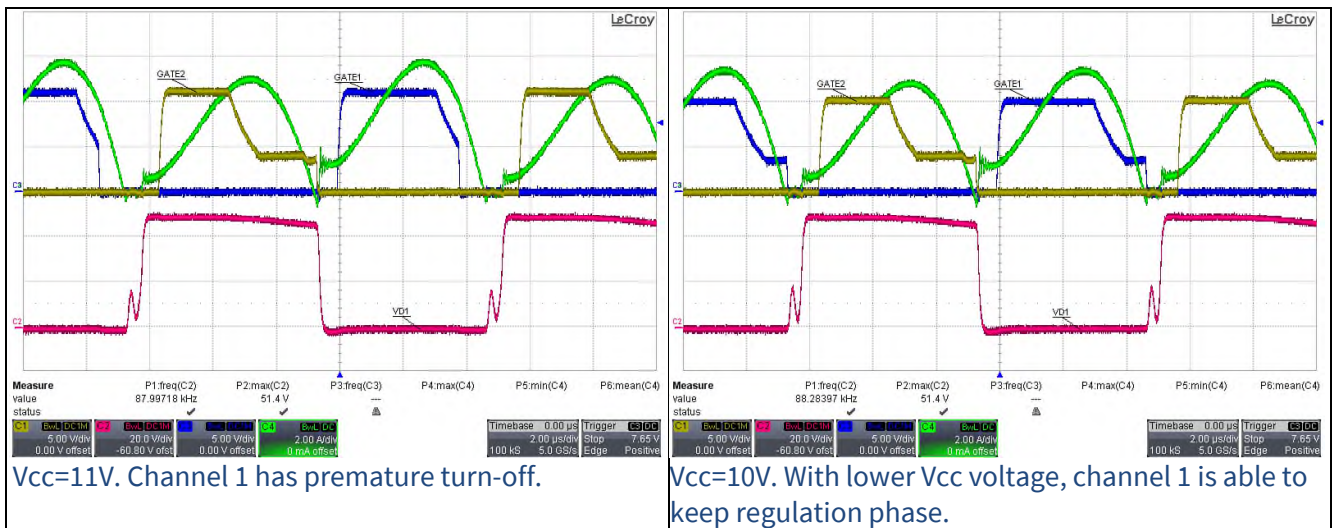
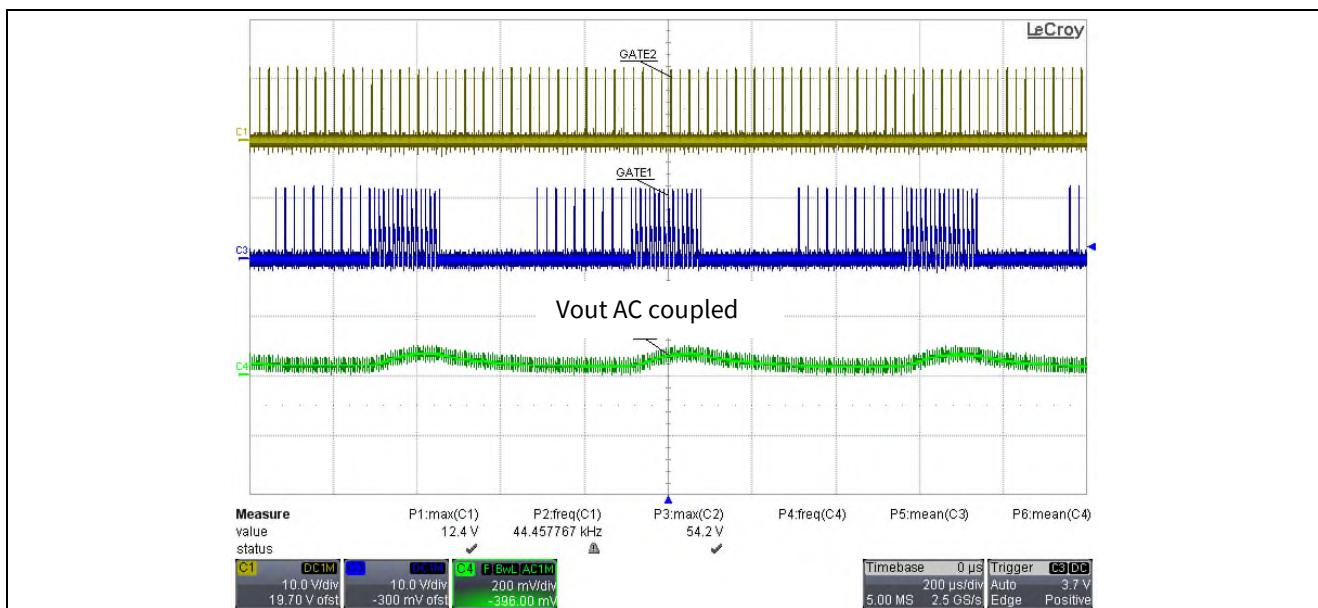


Figure 18 IR11688 gate regulation phase at different  $V_{CC}$  values

### 4.4 Light load ripple

One common issue encountered in LLC resonant converters with synchronous rectification, is the light load ripple. In a light load condition, the synchronous rectifier can show higher output ripple due to the burst mode switching that results from the SR driver IC operating intermittently as shown in figure 19:

Other application information



**Figure 19** Light load ripple due to intermittent gate drive

This happens because of the sinusoidal shape of the output current in an LLC resonant converter. The current in the SR MOSFET always rises from zero to its peak in the first half of the conduction phase and then drops to zero in the second half of conduction phase. At light load the output current is too low to hold the  $V_{DS}$  voltage more negative than  $V_{TH1}$  at the end of the MOT time. The IR11688 will therefore turn-off the gate drive immediately after MOT has expired, leaving the body diode to take over and carry the current for the rest of the conduction phase.

At the boundary load condition, the output current causes  $V_{DS}$  to be right around the  $V_{TH1}$  threshold at the end of MOT the time. The SR controller sees short conduction pulses for a few cycles, and enters MOT protection disabling the gate drive. After conducting through the body diode for the next few cycles the output voltage drops since body diode voltage drop is higher than channel  $R_{DSon}$  voltage drop. Conduction time then increases slightly to recharge the output capacitor and the cycle repeats resulting in higher than normal output voltage ripple. Intermittent gate drive output of the SR controller only happens at the boundary condition and is inherent in any controller with MOT protection. If the load is reduced further, the IR11688 will stay in MOT cycle skipping mode or totally disable gate output. At higher load, the IR11688 is able to turn-on for the full conduction time in every switching cycle.

Other application information

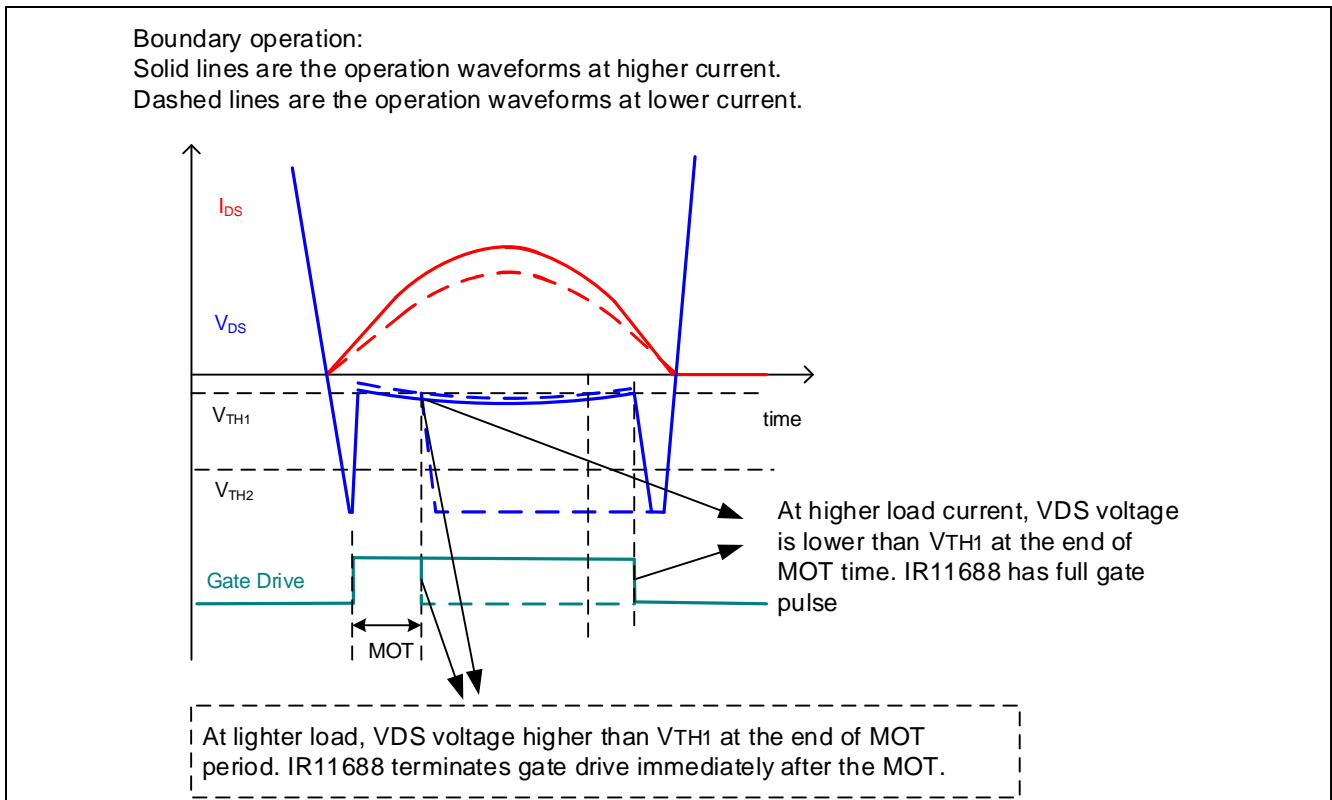


Figure 20 Light load ripple due to inconsistent gate drive

A solution is to set the MOT so that the boundary point will be at a current level as low as possible. At lower current output ripple can be managed to an acceptable level. To achieve this using earlier SR controllers such as the IR11682 it is necessary to add dynamic offset to the  $V_s$  pins in order to extend the effective minimum on time. However with IR11688 it can be done more easily by increasing the MOT resistor value to obtain the necessary minimum on time. The waveforms below show the same LLC converter at 1A load with MOT set to  $1\mu s$  and  $2\mu s$  respectively. It can be seen that extending the MOT effectively brings the IR11688 into steady operation. As a design rule of thumb, it is suggested to set the MOT between 25% and 40% of the switching period at  $f_{SWmax}$ .

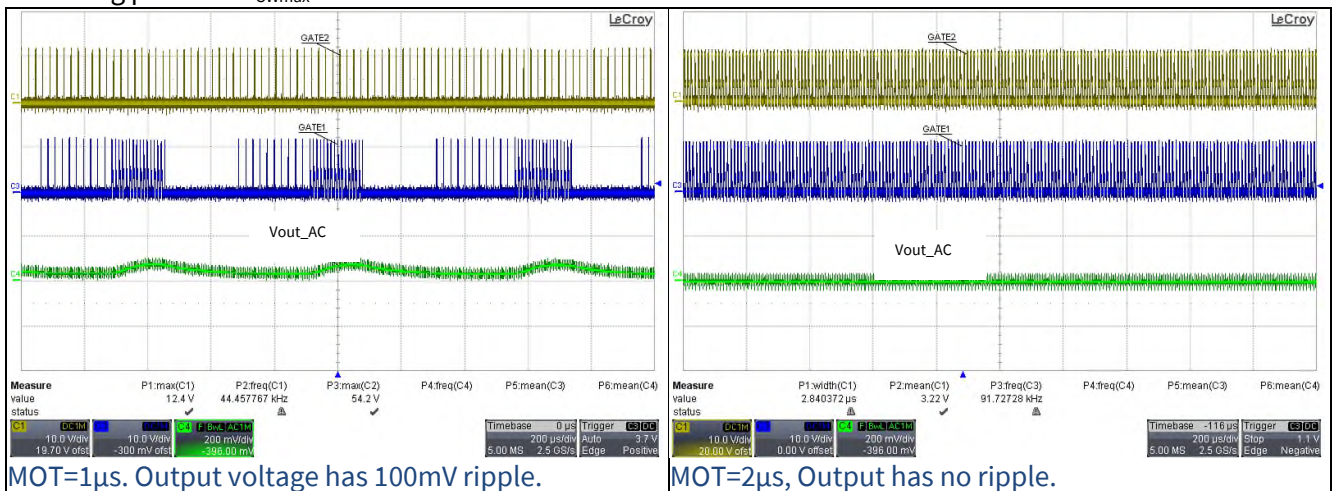


Figure 21 Effects of MOT setting

To fully eliminate this problem, it is suggested to disable the IR11688 at light load. This can be done by removing the  $V_{CC}$  supply.

Other application information

### 4.5 Gate clamping circuit for logic level MOSFET

The IR11688 is able to directly drive logic level MOSFETs. However if the  $dv/dt$  appearing at the drain is too high and the MOSFET Miller capacitance is large, voltage spikes reaching the gate threshold can be coupled from drain to gate. If this occurs before the SR control IC  $V_{CC}$  supply has risen sufficiently for it to be fully biased ( $V_{CC} < 2V$ ), the gate drive does not have sufficient pull down to prevent possible switch on. It is advised to pay close attention to the gate voltage of the SR MOSFET during system power up. If gate voltages above 2V are present, an external clamping circuit is recommended for logic level MOSFETs.

Figure 22 and 23 shows examples of clamping circuits. The PNP transistors are low voltage signal bipolar transistor (Figure 22); the clamp\_FETs are logic level signal MOSFET (Figure 23); both circuits could provide sufficient pull down current at low  $V_{CC}$ . PNP clamping circuit will affect IR11688 regulation feature. Signal MOSFET clamping circuit is recommended if the regulation feature is desired.

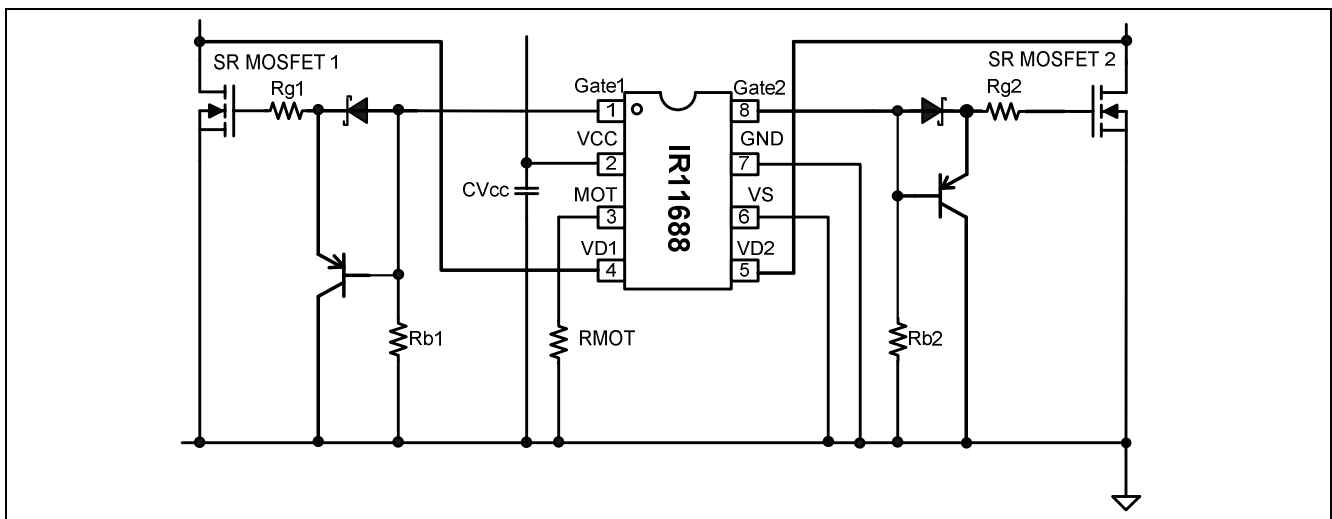


Figure 22 Gate clamping circuit for logic level MOSFET - PNP solution

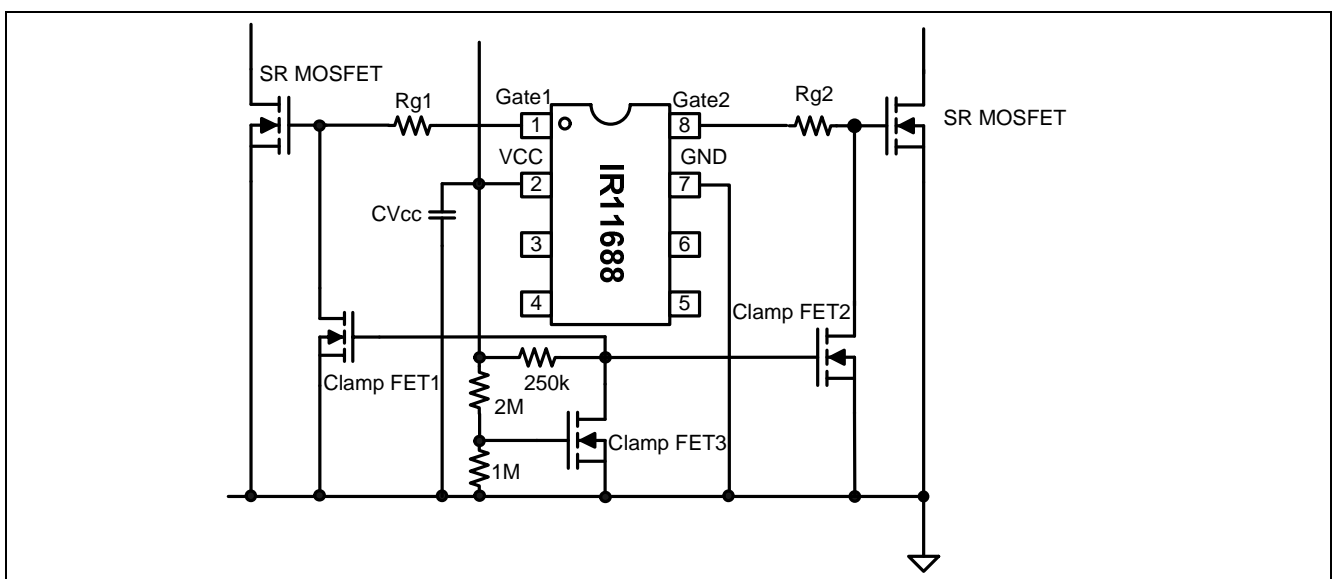


Figure 23 Gate clamping circuit for logic level MOSFET - signal MOSFET solution

## 5 SR MOSFET power loss calculation and MOSFET selection

The power loss in the SR MOSFET is the sum of conduction loss, switching loss, and gate driver loss.

The conduction loss of the IR11688 controlled synchronous rectifier can be broken down into body diode conduction loss, channel conduction loss, and regulation phase conduction loss. The conduction period is illustrated in Figure 24 where  $T_{b1}$  and  $T_{b2}$  are the body diode conduction phase,  $T_{con}$  and  $T_{reg}$  are the channel conduction phase.

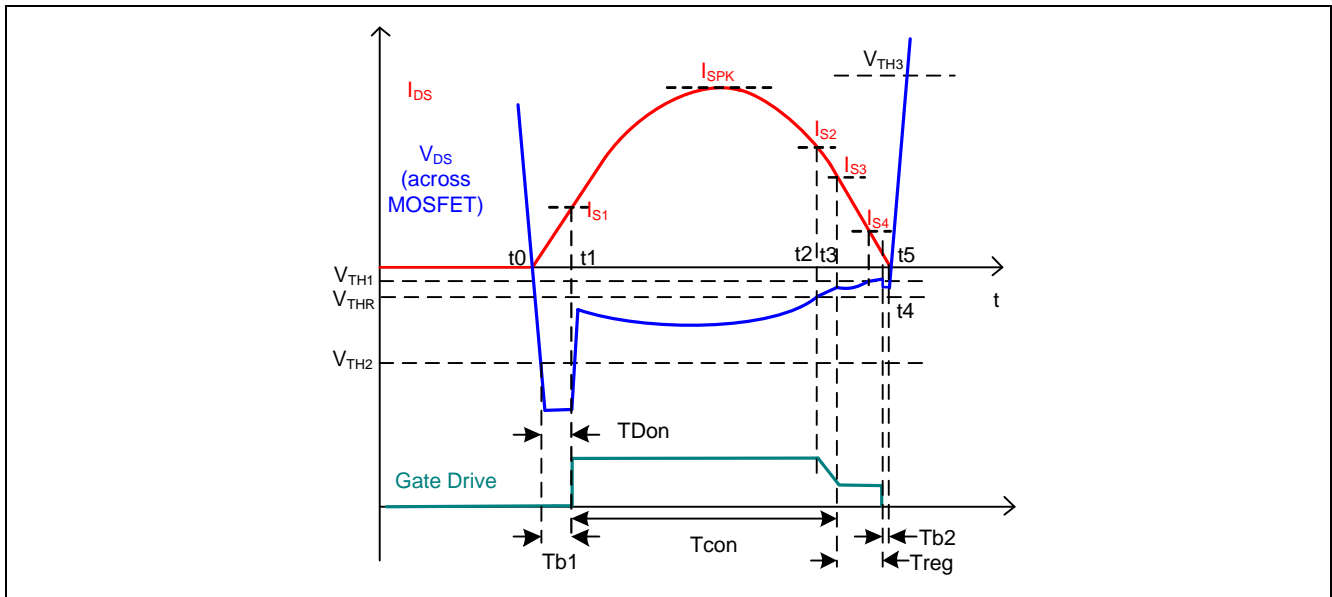


Figure 24 LLC sync rect waveform

### 5.1 Body diode conduction loss at turn-on

The power loss in the first body diode conduction phase can be calculated by:

$$P_{body1} = \frac{1}{2} \cdot T_{b1} \cdot f_{SW} \cdot V_F \cdot I_{S1} \quad (10)$$

$T_{b1}$  is approximate the turn-on propagation delay of the IR11688 ( $T_{Don}$  in the datasheet). If additional turn-on delay is applied in the circuit or a large gate resistor is used, the additional turn-on delay and gate rising time should be considered in  $T_{b1}$ .

$V_F$  is the body diode forward voltage drop.  $I_{S1}$  is the secondary current value at the time IR11688 gate turns on.  $I_{S1}$  can be estimated per the following equation:

$$I_{S1} = I_{SPK} \cdot \sin(2 \cdot \pi \cdot f_{SW} \cdot T_{b1}) \quad (11)$$

where  $I_{SPK}$  is the peak of secondary current,  $I_{SPK}$  is calculated by:

$$I_{SPK} = \frac{\pi}{2} \cdot I_{out} \quad (12)$$

and  $I_{out}$  is the average current of LLC converter.

The above calculation is based on an ideal sinusoidal current waveform when switching frequency is equal to resonant frequency. Actual secondary peak current is higher than this value when switching frequency is lower than resonant frequency (below resonant mode). In this case,

$$I_{S1} = I_{SPK} \cdot \sin(2 \cdot \pi \cdot f_r \cdot T_{b1}) \quad (13)$$

$$I_{SPK} = \frac{\pi}{2} \cdot I_{out} \cdot \frac{f_r}{f_{SW}} \quad (14)$$

## SR MOSFET power loss calculation and MOSFET selection

Where  $f_r$  is resonant frequency of LLC converter.  $f_r$  is defined by resonant inductor  $L_R$  and resonant capacitor  $C_R$ . Please see details in appendix: transformer leakage inductance and modeling.

### 5.2 Conduction loss in regulation phase

Before calculating MOSFET channel conduction loss, it is necessary to first review the conduction loss generated during the regulation phase. As explained in section 4.3, parasitic inductance in the  $V_{DS}$  sensing loop creates voltage offset. The offset voltage generated by parasitic/stray inductance can be calculated by the secondary current  $di/dt$  slope and the package stray inductance of MOSFET ( $L_{STRAY}$ ).

$$V_{OFFSET} = \frac{di}{dt} L_{STRAY} \quad (15)$$

The regulation phase starts at  $t_2$ , where secondary current drops to  $I_{S2}$ ,

$$I_{S2} = \frac{V_{THR} + V_{OFFSET}}{R_{DSon}} \quad (16)$$

$V_{THR}$  is the regulation threshold of the IR11688; the absolute value without a negative sign is used for this calculation.

In a normal SR conduction cycle, the regulation phase should happen during the second half of the sinusoid waveform, which is the falling slope. Thus the regulation phase starting time  $t_2$  is calculated by:

$$t_2 = \frac{\pi - \arcsin\left(\frac{I_{S2}}{I_{SPK}}\right)}{\pi \cdot 2 \cdot f_r} \quad (17)$$

At  $t_2$ , gate voltage starts to be discharged by the IR11688. At time  $t_3$ , the gate voltage is low enough to maintain the regulation of  $V_{DS}$  at -50 mV. The discharging time ( $t_3 - t_2$ ) is determined by the SR MOSFET equivalent SYNC capacitance  $C_{sync}$ , and the gate threshold voltage where drain-source resistance drops rapidly. As a general guide, the  $V_{GS}$  voltage that gives 2x of rated  $R_{DSon}$  can be used for the calculation ( $V_{GS2}$ ). This voltage can be found in MOSFET datasheet in a plot of  $R_{DSon}$  vs.  $V_{GS}$ .

$$t_3 - t_2 \approx 150 \cdot C_{sync} \cdot \ln\left(\frac{V_{cc}}{V_{GS2}}\right) \quad (18)$$

$$t_3 \approx t_2 + 150 \cdot C_{sync} \cdot \ln\left(\frac{V_{cc}}{V_{GS2}}\right) \quad (19)$$

MOSFET current at  $t_3$  is then derived by:

$$I_{S3} = I_{SPK} \cdot \sin(2 \cdot \pi \cdot f_r \cdot t_3) \quad (20)$$

The power loss at regulation phase is:

$$P_{reg} = \frac{1}{2} (t_5 - t_3) \cdot f_{SW} \cdot I_{S3} \cdot (V_{THR} + V_{OFFSET}) \quad (21)$$

$$t_5 = \frac{1}{2 \cdot f_r} \quad (22)$$

### 5.3 Channel conduction loss

To simplify the channel conduction loss calculation, it is assumed that the MOSFET is turned on during the whole half of switching cycle. The RMS current in each branch of the synchronous rectifier is half of the peak current that calculated in the previous stage.

SR MOSFET power loss calculation and MOSFET selection

$$I_{SRMS} = \frac{I_{SPK}}{2} \tag{23}$$

$$P_{con1} = I_{srms}^2 \cdot R_{DSon} \tag{24}$$

$R_{DSon}$  is MOSFET channel on state resistance.  $R_{DSon}$  (normally shown in the datasheet) at 25°C is approximately 1.5 times higher at  $T_j=100^\circ\text{C}$ . Proper temperature coefficient should be considered in channel conduction loss calculation.

### 5.4 Body diode conduction loss at turn-off

If regulation phase works properly, the body diode conduction phase at turn-off is very short and the power loss is negligible.

### 5.5 Switching loss

The switching loss is different in DCM mode and CCM mode. For DCM, only the below-resonant operation at heavy load is of interest and is discussed here.

Figure 25 is a typical DCM waveform for switching below resonance (refer to Figure 2).  $V_s$  is the primary switching node voltage,  $V_{C_R}$  is the primary resonant capacitor voltage,  $I_{L_R}$  is the primary current,  $I_{L_m}$  is the primary magnetizing current,  $I_{SR1}$  and  $I_{SR2}$  are the output current in each SR MOSFET and  $V_{DS1}$  is the Drain to Source voltage of SR MOSFET MSR1. At the end of each SR conduction cycle, the sinusoidal current reduces to zero and the SR MOSFET is turned off by the IR11688. When the switching frequency is below the resonant frequency, at the end of the conduction cycle the primary voltage has not changed polarity, therefore the SR MOSFETs of both channels remain in the off state and the  $V_{DS}$  voltage exhibits ringing oscillations.

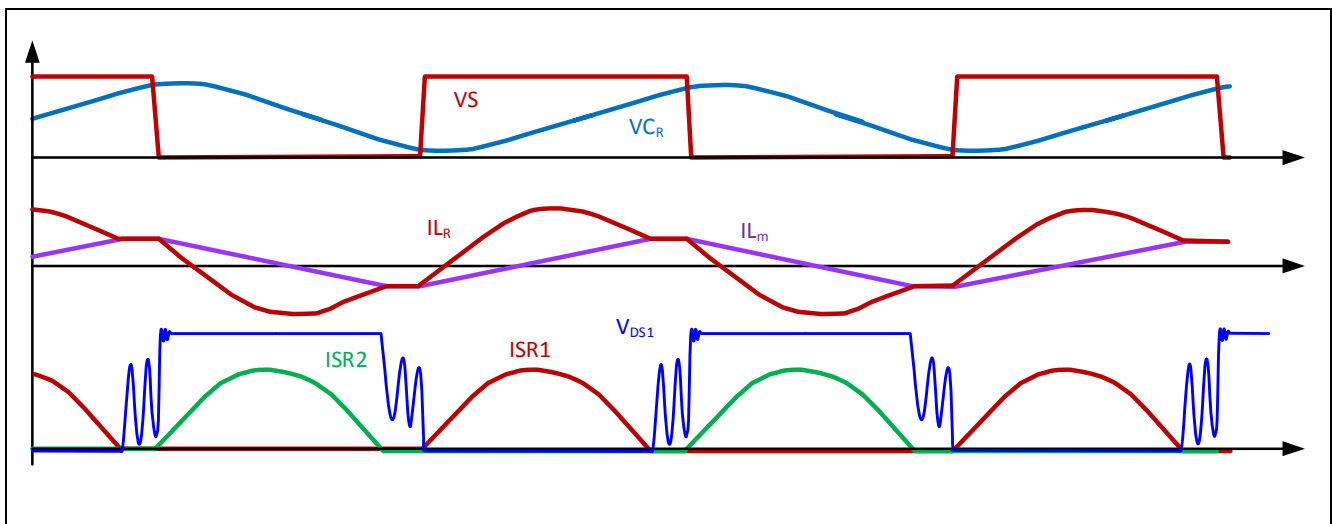


Figure 25 LLC below resonant DCM waveform

Figure 26 details the waveform of one SR cycle in below resonance DCM. From  $t_0$  to  $t_1$ , power is delivered from transformer to load,  $t_1-t_0$  duration equals to half of the resonant period. At  $t_1$ , the resonant inductor current  $I_{L_R}$  meets the transformer magnetizing current  $I_{L_m}$  and secondary current reduces to zero. During  $t_1$  to  $t_2$ , two resonant actions occur resulting from; firstly, primary side resonant inductor  $L_R$ , magnetizing inductance  $L_m$  resonating with  $C_R$  and secondly, the resonant inductor  $L_R$  resonating with secondary side SR MOSFET  $C_{oss}$ . As  $C_R$  is much larger than SR MOSFET  $C_{oss}$ ,  $V_{C_R}$  can be considered constant during  $t_1-t_2$ . The secondary high frequency oscillation during  $t_1-t_2$  is defined by:

SR MOSFET power loss calculation and MOSFET selection

$$Fr3 = \frac{1}{2\pi\sqrt{L_R/n^2 \cdot (2 \cdot Coss_s)}} \tag{25}$$

Where  $L_R = L_{R3}$  is the primary leakage inductance measured with all secondary winding shorted (refer to Appendix),  $n$  is transformer turns ratio and  $Coss_s$  is Sync Rect MOSFET output capacitance. The equivalent resonant circuit is shown in Figure 27. The negative resonant current is defined by the body diode reverse recovery performance under the  $di/dt$  at  $t1$ . Please note the reverse recovery charge is usually much smaller than  $Qrr$  specified in the MOSFET datasheet as the  $di/dt$  and forward current in body diode are both smaller than datasheet test condition. During the resonance period, only small power loss drops on resistive components in the loop such as transformer ESR.

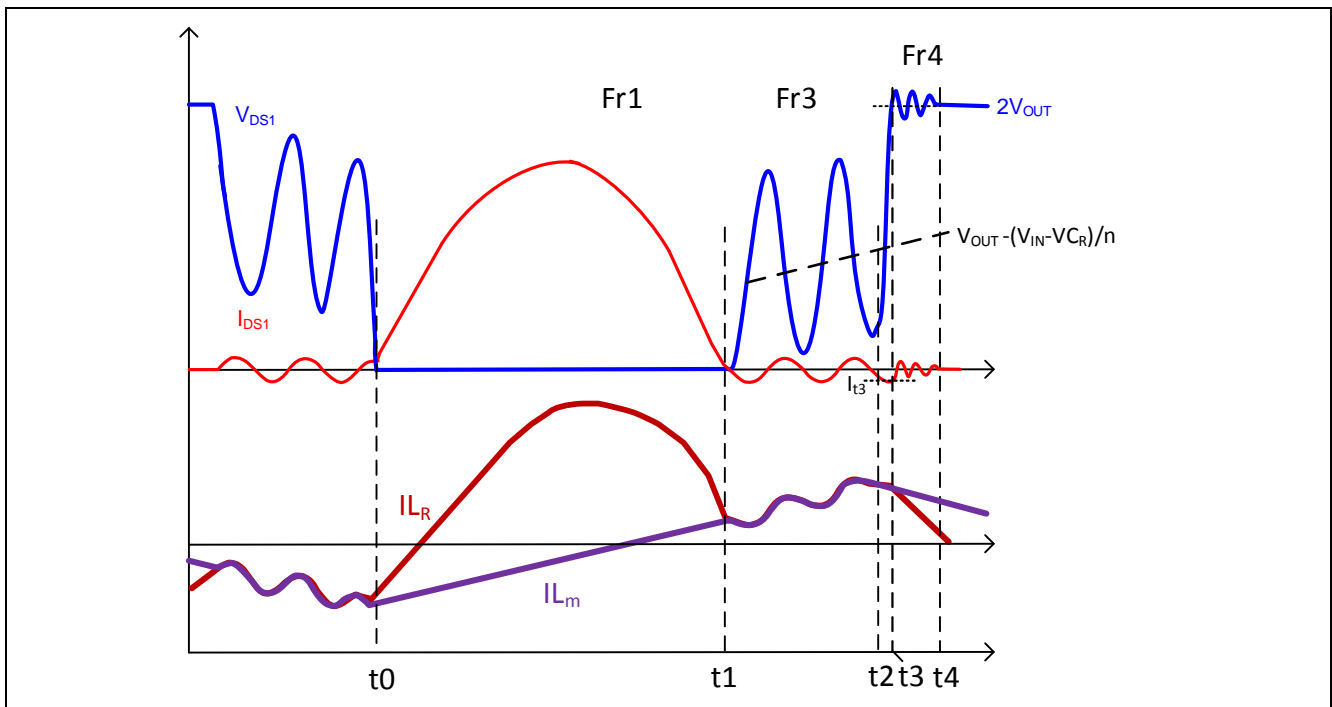


Figure 26 LLC DCM SR waveform of MSR1

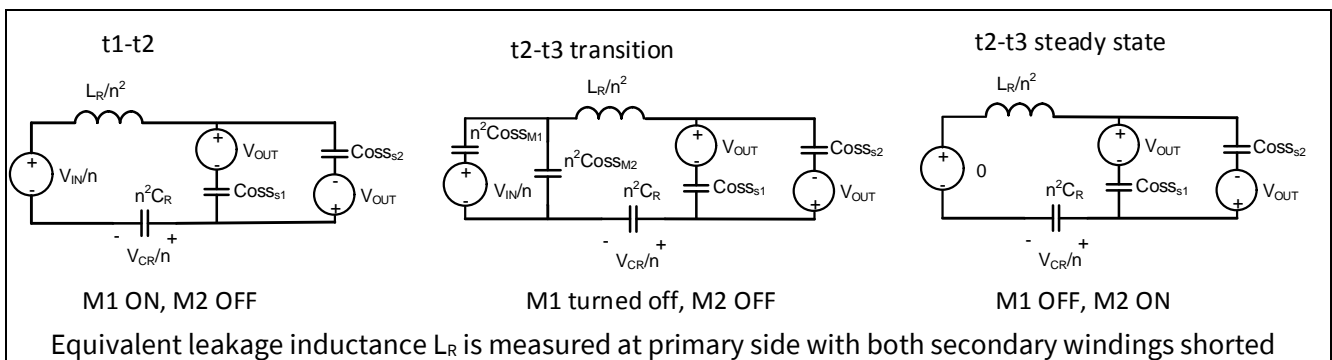


Figure 27 Equivalent circuit of DCM during  $t1-t2$  and  $t2-t3$

At  $t2$ , the primary high-side MOSFET M1 switch off, the transformer magnetizing current  $I_{Lm}$  starts charging the parasitic output capacitor of M1, while discharging  $C_{OSS}$  of M2.  $I_{Lm}$  can be considered as a constant current source during the transition. Primary dead-time can be calculated per  $I_{Lm}$  and  $C_{OSS}$  of M1 and M2. The dead-time should be longer than the  $C_{OSS}$  charging/discharging time to guarantee ZVS operation. At time  $t2$ , the secondary  $V_{DS1}$  voltage could be anywhere between  $0V$  and  $2(V_{OUT} - (V_{IN} - V_{CR})/n)$  depending on the resonant oscillation phase at  $t2$ . The  $I_{DS1}$  current at  $t2$  always drops to negative due to negative  $di/dt$  applied. When the voltage at the  $V_s$  node drops to  $0V$ , the secondary equivalent circuit in  $t2-t3$  behaves very similarly



SR MOSFET power loss calculation and MOSFET selection

$I_{D\_CCM1}$ . The IR11688 may or may not turn off MSR1 at  $t_1$  so either the channel or the body diode of MSR1 conducts current. The transformer secondary voltage is still clamped to  $V_{OUT}$ . The whole  $V_S$  voltage swing ( $V_{IN}$ ) is dropped across the resonant inductor  $L_R$  to generate negative  $di/dt$ . The  $di/dt$  slope during  $t_1$  to  $t_2$  is defined by:

$$\frac{di_{LR}}{dt} = \frac{V_{IN}}{L_R} \tag{30}$$

$$\frac{di_{DS}}{dt} = n \cdot \left( \frac{V_{IN}}{L_R} + \frac{n \cdot V_{OUT}}{L_m} \right) \tag{31}$$

The IR11688 will turn-off MSR1 as soon as the  $V_{DS1}$  voltage reaches  $V_{TH1}$ . The turn-off threshold can be calculated by the following equation.

$$I_{D\_CCM2} = \frac{V_{TH1} + \frac{di_{DS}}{dt} \cdot L_{STRAY}}{R_{DSon}} - \frac{di_{DS}}{dt} \cdot T_{Doff} \tag{32}$$

Where,  $T_{Doff}$  is IR11688 turn-off propagation delay.

It is worth mentioning that here the  $R_{DSon}$  could be larger than specified in the datasheet as the IR11688 would usually be in regulation mode during turn-off.

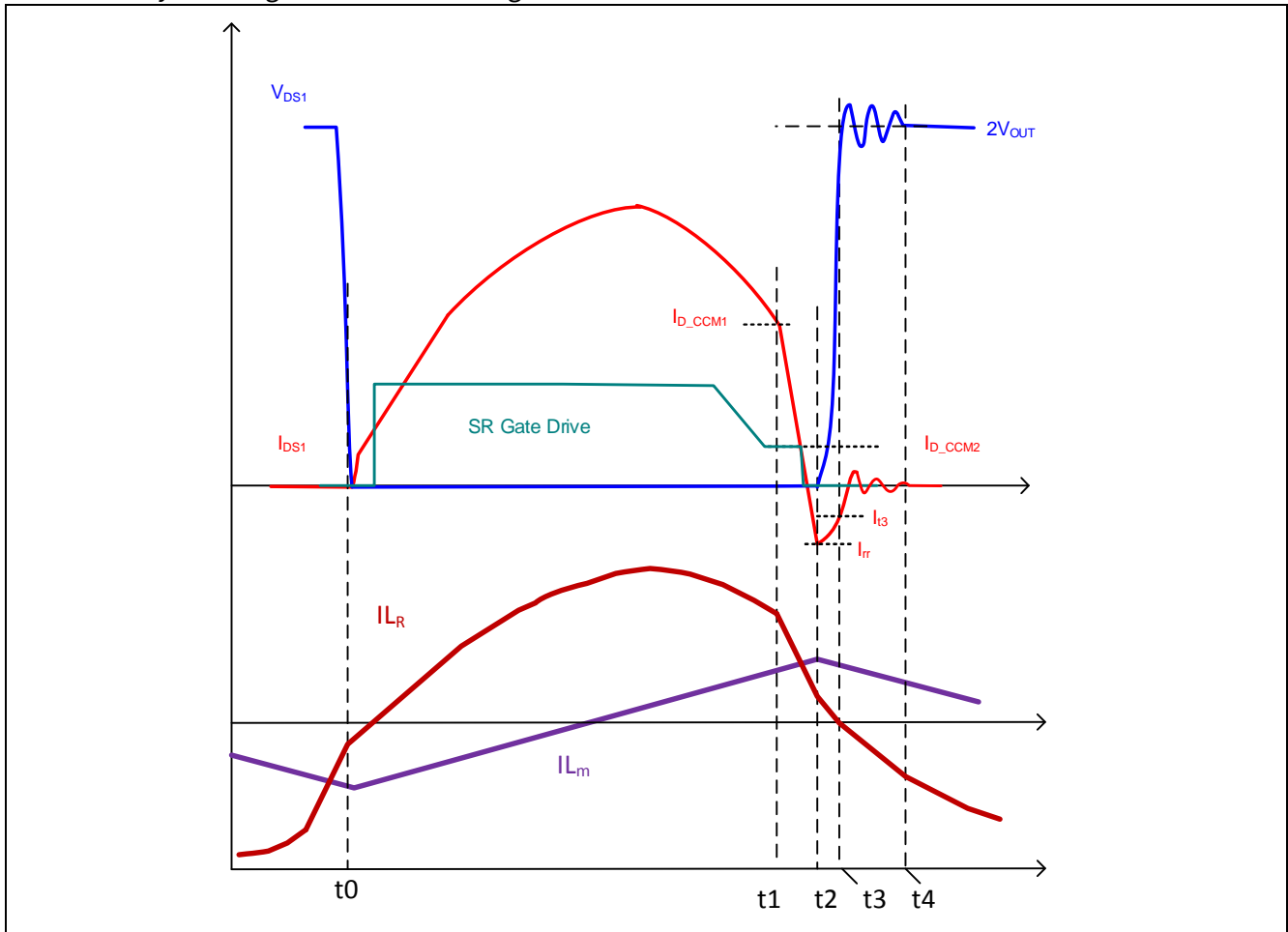


Figure 29 LLC CCM SR waveform of MSR1

When the MSR1 channel is turned off,  $I_{DS}$  current transfers to its body diode. The body diode will continue carrying current to negative  $I_{rr}$  until all the stored charges have been removed. At  $t_2$ , the body diode starts blocking voltage.  $I_{rr}$  is determined by initial current  $I_{D\_CCM2}$ , the  $di_{DS}/dt$  @  $t_1$ - $t_2$ , and the  $V_{OUT}$  voltage. Again usually this value is not available in MOSFET datasheets as the application condition is different to the JEDEC test condition.

SR MOSFET power loss calculation and MOSFET selection

From t2 to t3,  $C_{oss}$  resonates with the equivalent leakage inductance  $L_R$  reflected to the secondary. The resonant frequency at t2-t3 is Fr3 (equation 25).  $V_{DS1}$  voltage rises towards  $2V_{OUT}$ . This is the same as in DCM mode. As long as  $V_{DS1}$  exceeds twice the output voltage, the opposite winding forces the counterpart SR MOSFET MSR2 to conduct current. Fr3 resonance then stops and Fr4 resonance begins. Energy stored in the parasitic inductance creates a voltage spike on  $V_{DS1}$ .

$$V_{SPIKE} = 2 \cdot V_{OUT} + \sqrt{\frac{L_{paras} \cdot I_{t3}^2}{C_{OSS}}} \tag{33}$$

The energy stored in the parasitic inductance will dissipate in the SR MOSFET, transformer ESR and in the load. The switching loss in SR MOSFET is estimated:

$$P_{SW} < \frac{1}{2} L_{paras} \cdot I_{t3}^2 \cdot f_{sw}; I_{t3} \text{ is SR current measured at } V_{DS}=2V_{OUT} \tag{34}$$

### 5.6 Gate charge loss

The total gate driver loss is discussed in section 3.4.  $P_{R_{gext}}$  is used to calculate the gate drive loss dissipated in the MOSFET:

$$P_{R_{gFET}} = \frac{R_{gFET}}{R_g} P_{R_{gext}} \tag{35}$$

$R_{gFET}$  is the internal gate resistance of the SR MOSFET and  $R_g$  is the external gate resistor.

Total power loss in the SR MOSFET is therefore:

$$P_{FET} = P_{body1} + P_{reg} + P_{con} + P_{sw} + P_{R_{gFET}} \tag{36}$$

### 5.7 MOSFET selection guide

In LLC application, both turn-on and turn-off of SR MOSFET are in ZVS and are nearly in ZCS.  $C_{oss}$  is charged by resonant circuit, not by voltage source. Conduction loss dominates and switching loss is minimal. The key parameters that affect performance are  $R_{DSon}$  and  $Q_{sync}$ . Usually lower  $R_{DSon}$  results in lower conduction loss. However, keep in mind IR11688 control scheme is based on  $V_{DS}$  sensing. Lower  $R_{DSon}$  would trigger IR11688 switch-off MOSFET at a higher current level and lead to higher conduction loss due to body diode. As rule of thumb, it is suggested choosing  $R_{DSon}$  at around 50 mV/Iout.

## 6 PCB layout guidelines and examples

### IC placement

Due to the nature of the control based on fast and accurate voltage sensing, it is essential to lay out the circuit keeping the IR11688 as close as possible to the SR MOSFETs. As a general guideline, the physical distance between the two devices should not exceed 10 mm (0.4 inches).

### IC decoupling capacitor

The key element to properly decoupling the IC is the physical location of the  $V_{CC}$  capacitor and its connections to the power terminals. In order for this capacitor to provide effective filtering, it must be located as close as physically possible to the  $V_{CC}$  and COM pins and connected through the shortest available path.

### Gate drive loop

Minimal gate drive loop will reduce requirements for damping and enhance system robustness. Gate loop inductance plays a major role in damping requirements. Once layout is finalized, then a “rule of thumb” estimation consists of measuring the physical loop trace length, assuming each millimeter (1 mm = 39.37 mils) to add 1 nH of inductance. Other methods include measurement (low frequency RCL meters or current slope for a given voltage pulse) or FEM simulations.

### MOT resistor

The MOT resistor should be placed as close as possible to the MOT pin and GND pin. It should use a separate signal ground trace star-connected to the GND pin.

### $V_S$ connection

$V_S$  pin is the differential sense pin for internal  $V_{DS}$  comparators. This pin should be Kelvin connected to the Source of SR MOSFETs. If the two SR MOSFETs are apart from each other, connect  $V_S$  to the Source of channel 2 MOSFET. Avoid connecting  $V_S$  directly to GND pin (pin7).

PCB layout guidelines and examples

Double layer board layout examples are shown in the following figures:

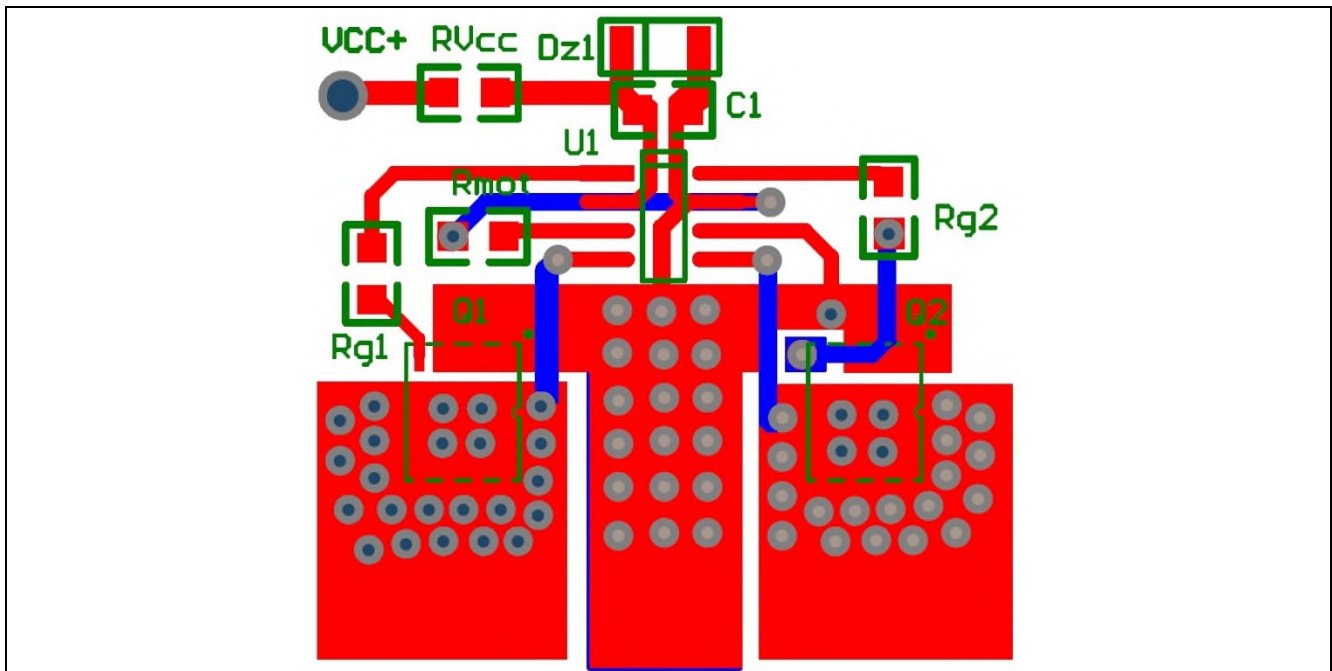


Figure 30 Single layer layout example with QFN MOSFET

Thermal vias are added to the QFN package to transfer heat from the top of PCB to the bottom layer.

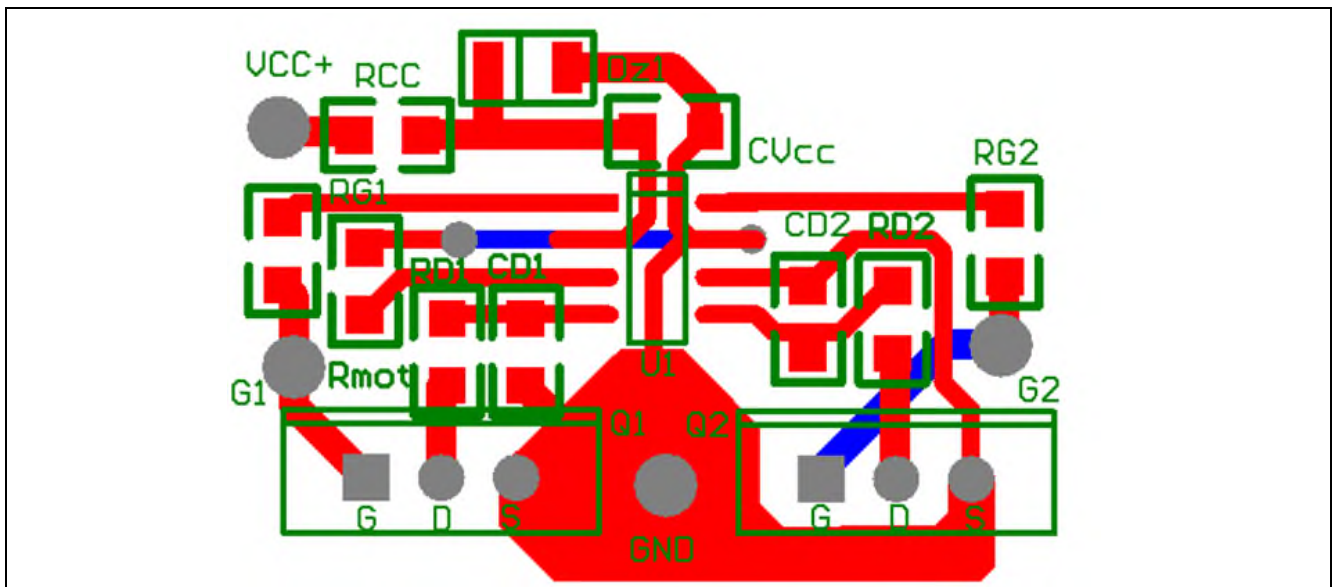


Figure 31 Single layer PCB example with TO-220 MOSFET

Add RC filter to VD pin when necessary to avoid DCM ringing false trigger IR11688

## 7 Appendix: Transformer leakage inductance and modeling

The physical model of a transformer with one primary winding and two symmetrical secondary windings (i.e. center-tapped secondary) is shown as Figure 32.  $L_m$  is transformer magnetizing inductance,  $L_{KP}$  is transformer primary leakage inductance,  $L_{KS1}$  and  $L_{KS2}$  are transformer secondary leakage inductance. Leakage inductance indicates flux is not coupled between primary and secondary.

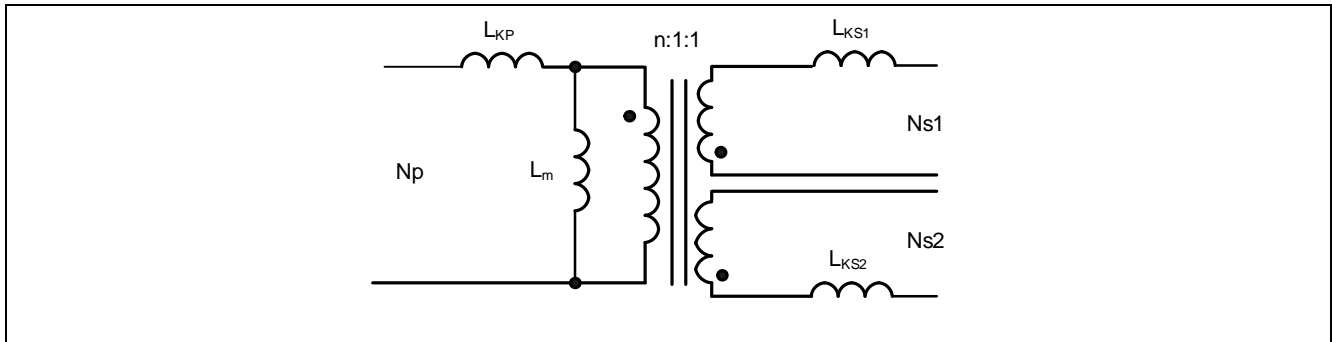


Figure 32 Transformer model

Figure 33 is a typical LLC circuit with simplified transformer model.  $L_R$  is resonant inductor and  $C_R$  is resonant capacitor.  $L_R$  and  $C_R$  define resonant frequency  $F_{r1}$ .

$$F_{r1} = \frac{1}{2\pi\sqrt{L_R \cdot C_R}}$$

$L_R$  could be an external inductor or in many cases the leakage inductance of transformer. Here to simplify the statement, we take the second scenario: the resonant inductor is purely contributed by transformer leakage inductance.

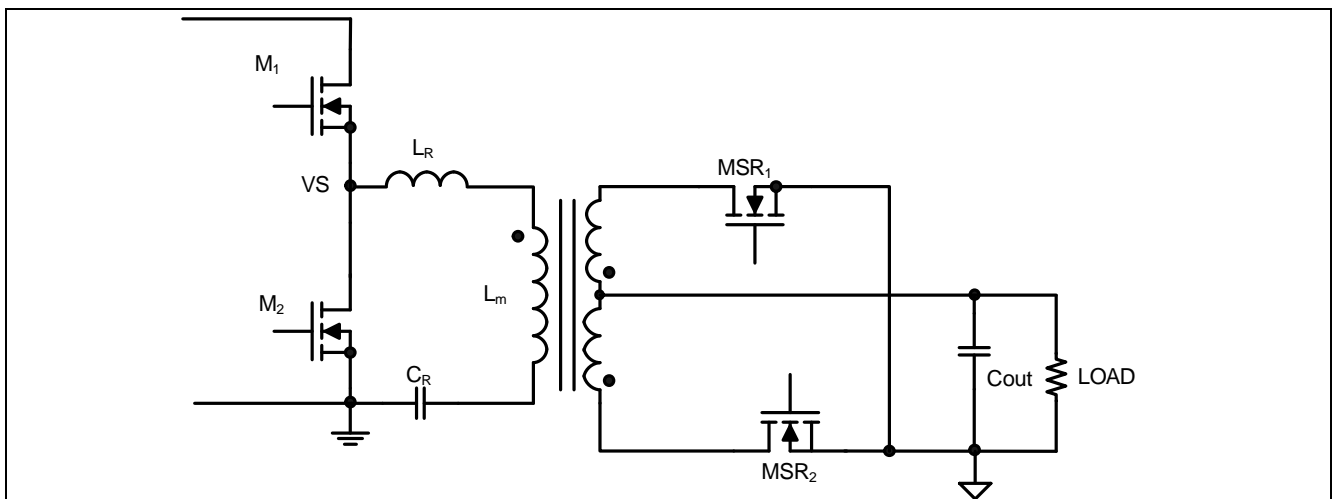


Figure 33 Typical LLC circuit

It is a general practice that leakage inductance is measured at the primary winding terminals with all secondary windings shorted. This leakage inductance includes the physical primary leakage inductance  $L_{KP}$  and physical secondary leakage inductance that reflected to primary. As mentioned, the leakage inductance is usually measured with all secondary windings shorted. This common practice however is not accurate and introduces error to the resonant circuit design.

Take the power delivery phase as an example. It happens when one secondary winding is conducting current; illustrated as Figure 34 (a). For AC analysis, output capacitor is considered short circuit. So we have

Appendix: Transformer leakage inductance and modeling

one secondary winding N<sub>s1</sub> in short and the other secondary winding N<sub>s2</sub> open. From the terminal of N<sub>p</sub>, it sees N<sub>p</sub> leakage inductance L<sub>KP</sub>, in series with magnetizing inductance L<sub>m</sub>, which is in parallel with reflected N<sub>s1</sub> leakage inductance n<sup>2</sup>L<sub>KS1</sub>. Please refer to Figure 34 (b). This is the actual inductance that resonant with C<sub>R</sub> and creates sinusoid current shape. Thus the correct measurement of primary leakage inductance should be: measure primary winding inductance with only one of the secondary winding shorted.

$$L_{R1} = L_{KP} + \frac{L_m \cdot n^2 \cdot L_{KS1}}{L_m + n^2 \cdot L_{KS1}}, \text{ Np inductance when Ns1 is shorted}$$

$$L_{R2} = L_{KP} + \frac{L_m \cdot n^2 \cdot L_{KS2}}{L_m + n^2 \cdot L_{KS2}}, \text{ Np inductance when Ns2 is shorted}$$

The two leakage inductance L<sub>R1</sub> and L<sub>R2</sub> could be identical if the two secondary windings are exactly symmetric in physical location and size. If they have the same coupling to primary, we will get L<sub>R</sub>=L<sub>R1</sub>=L<sub>R2</sub>. In reality, it is always difficult to put secondary windings symmetric. Then each secondary winding will have its own resonant frequency in its active half cycle. This could result in unbalance current in two secondary windings. The resonant frequency Fr1 is defined by:

$$F_{r1\_1} = \frac{1}{2\pi\sqrt{L_{R1} \cdot C_R}}$$

$$F_{r1\_2} = \frac{1}{2\pi\sqrt{L_{R2} \cdot C_R}}$$

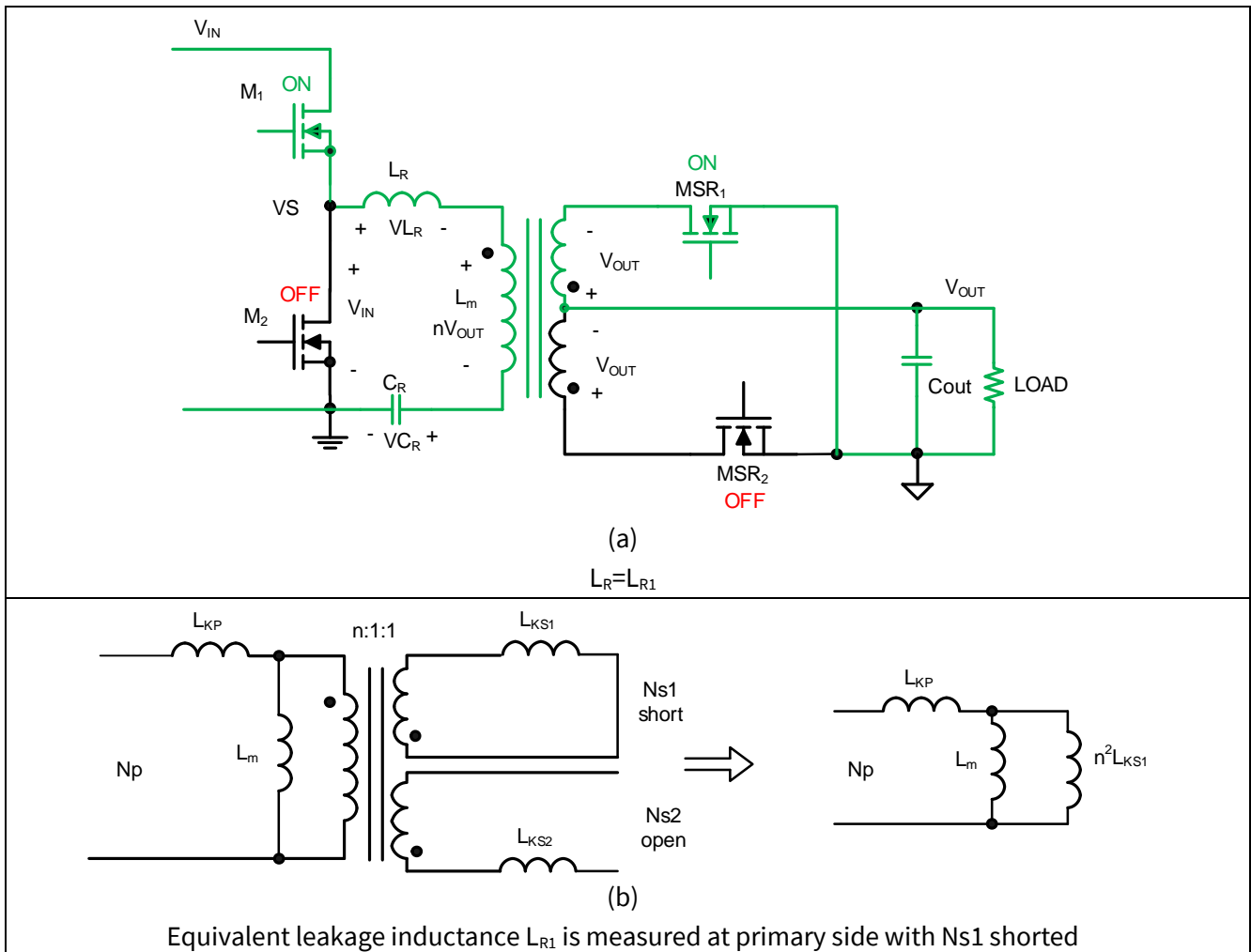


Figure 34 Equivalent transformer model in resonant (one secondary winding in conduction mode)

The following equations can be used to calculate each of the physical inductance in Figure 32.

Appendix: Transformer leakage inductance and modeling

$L_P = L_{KP} + L_m$ , measure primary inductance with all secondary windings open

$L_{R1} = L_{KP} + \frac{L_m \cdot n^2 \cdot L_{KS1}}{L_m + n^2 \cdot L_{KS1}}$ , measure primary inductance with Ns1 short

$L_{R2} = L_{KP} + \frac{L_m \cdot n^2 \cdot L_{KS2}}{L_m + n^2 \cdot L_{KS2}}$ , measure primary inductance with Ns2 short

$L_{S1} = L_{KS1} + \frac{L_m}{n^2}$ , measure secondary Ns1 inductance with all windings open

$L_{S2} = L_{KS2} + \frac{L_m}{n^2}$ , measure secondary Ns2 inductance with all windings open

To simplify calculation, assume Ns1 and Ns2 are symmetric and have identical magnetizing inductance and leakage inductance.  $L_R=L_{R1}=L_{R2}$ ,  $L_{KS1}=L_{KS2}=L_{KS}$ ,  $L_{S1}=L_{S2}=L_S$ .

$$L_R = L_{KP} + \frac{L_m \cdot n^2 \cdot L_{KS}}{L_m + n^2 \cdot L_{KS}}$$

$$L_S = L_{KS} + \frac{L_m}{n^2}$$

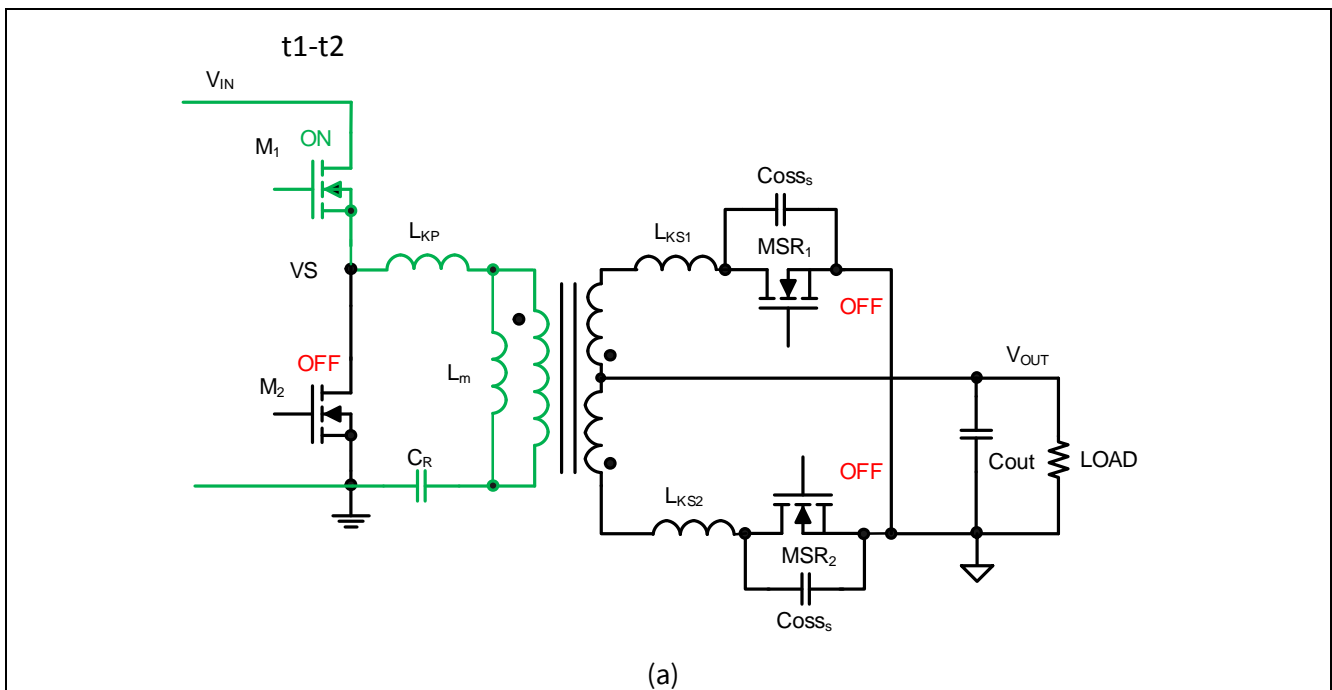
$$L_P = L_{KP} + L_m$$

Three unknowns, three equations, puzzle could be solved. The values could be verified with more measurement. For example secondary leakage inductance can be measured with primary winding  $N_p$  shorted.

$$L_{RS1} = L_{KS1} + \frac{1}{n^2} \frac{L_{KP} \cdot L_m}{L_m + L_{KP}}$$
, Ns1 leakage inductance measured with  $N_p$  shorted

Once we have the parameters of a transformer, we can analyze other operation mode. Figure 35 is the equivalent circuit of DCM resonant in  $t_1$ - $t_2$  interval that mentioned in chapter 5.5. In this mode, both secondary switches are open. Transformer leakage inductor, magnetizing inductor, resonant capacitor  $C_R$  and SR MOSFET output capacitor form resonant circuit. The equivalent circuit of transformer is shown in Figure 35(b). The equivalent leakage inductance in this mode can be measured at primary side with both secondary windings shorted.

$$L_{R3} = L_{KP} + L_m // (n^2 \cdot L_{KS1}) // (n^2 \cdot L_{KS2})$$
, primary leakage inductance with Ns1 and Ns2 shorted



Appendix: Transformer leakage inductance and modeling

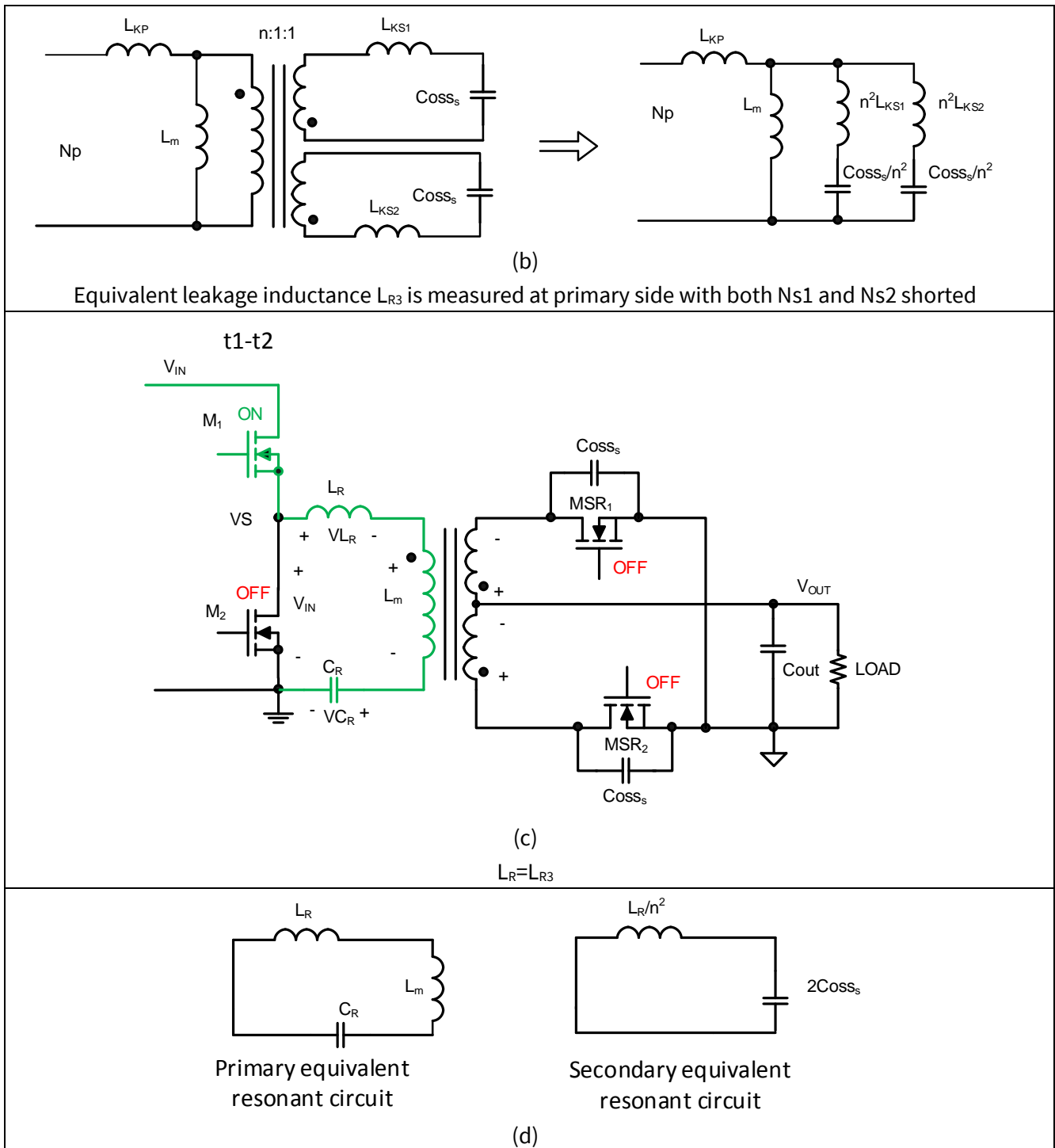


Figure 35 Equivalent transformer model in DCM (t1-t2) of Figure 26

It has two resonant circuits. The first resonant circuit is at primary side:  $L_R$ ,  $L_m$  resonant with  $C_R$  at a very low frequency.

$$Fr2 = \frac{1}{2\pi\sqrt{(L_{R3} + L_m) \cdot C_R}}$$

The second resonant frequency is determined by:

$$Fr3 = \frac{1}{2\pi\sqrt{L_{R3}/n^2 \cdot (2 \cdot C_{oss_s})}}$$

---

**Appendix: Transformer leakage inductance and modeling**

Another important leakage inductance is the leakage between two secondary windings. This leakage inductance can be measured at N<sub>s1</sub> with N<sub>s2</sub> shorted, vice versa. Here name as L<sub>KS1-2</sub> and L<sub>KS2-1</sub>. For symmetric secondary, L<sub>KS1-2</sub> equals L<sub>KS2-1</sub>. Again this is the total equivalent secondary leakage inductance that physically presents at both N<sub>s1</sub> and N<sub>s2</sub>. In the model we could simply split it equally to N<sub>s1</sub> and N<sub>s2</sub>. In most conditions, L<sub>KS1-2</sub> and L<sub>KS2-1</sub> are too small to affect operation and can be ignored. However, during the turn-off of secondary switch, energy stored in L<sub>KS1-2</sub> and L<sub>KS2-1</sub> create voltage spike on V<sub>DS</sub> of SR MOSFET. It is necessary to have L<sub>KS1-2</sub> and L<sub>KS2-1</sub> available for switching loss calculation. Here gives the example of MSR1.

$$P_{SW} = \frac{1}{2} L_{paras} \cdot I_{t3}^2 \cdot f_{sw}$$

$$L_{paras} = L_{KS1-2} + L_{stray} + L_{PCB}$$

$$Fr4 = \frac{1}{2\pi\sqrt{L_{paras} \cdot Coss_s}}$$

L<sub>stray</sub> is SR MOSFET package inductance, L<sub>PCB</sub> is PCB trace inductance, I<sub>t3</sub> is the current in MSR1 at time t<sub>3</sub> (Figure 26, Figure 29).

Based on above, we know the equivalent leakage inductance of LLC transformer is not a constant value. It varies with operating mode. Resonant frequency should be calculated with the corresponded leakage inductance in that specific mode.

## 8 Appendix: Symbols list

### Symbols list <sup>[1]</sup>

$V_{TH1}$ : IR11688 turn-off threshold

$V_{TH2}$ : IR11688 turn-on threshold

$V_{TH3}$ : IR11688 periodic logic (reset) threshold

$V_{THR}$ : IR11688 turn-off regulation threshold

$T_{Don}$ : IR11688 turn on propagation delay

$T_{Doff}$ : IR11688 turn off propagation delay

$R_{Dson}$ : synchronous rectifier MOSFET channel ON resistance

$I_D$ : synchronous rectifier MOSFET drain current

$V_{DS}$ : synchronous rectifier MOSFET drain to source voltage

MOT: IR11688 minimum ON time parameter

$t_{blank}$ : IR11688 turn off blanking time

$C_{dc}$ : IR11688 decoupling capacitor on  $V_{cc}$

$R_{g1,2}$ : SR MOSFET gate drive loop resistance external to IR11688 IC

$R_{CC}$ : supply voltage series resistor value ( $V_{supply}$  to  $V_{CC}$ )

$f_{sw}$ : converter switching frequency

$f_{sw,max}$ : converter maximum operating switching frequency

$Q_g$ : SR MOSFET total gate charge

$Q_{gd}$ : SR MOSFET gate to drain (Miller) charge

$Q_{gs}$ : SR MOSFET gate to source charge

$L_g$ : total gate loop parasitic inductance

$C_{iss}$ : SR MOSFET input capacitance

$V_m$ : Miller plateau voltage of MOSFET

$C_{sync}$ : SR MOSFET equivalent input capacitance in ZVS mode

$P_{dr}$ : Total power dissipated by the gate drive function for each SR MOSFET

$R_{source}$ : gate driver source resistance

$R_{sink}$ : gate driver sink resistance

$P_{Rg}$ : Power dissipated in each gate resistor

$P_{IC}$ : IR11688 IC maximum power dissipation

$V_{CC}$ : Supply voltage on IR11688  $V_{cc}$  pin

$I_{CC}$ : IR11688 IC supply current

$L_R$ : LLC resonant inductance

$C_R$ : LLC resonant capacitor

$n$ : transformer turns ratio

[1] IR11688 SmartRectifier™ control IC datasheet



---

Appendix: Symbols list

## Revision History

Major changes since the last revision

Page or Reference	Description of change
--	First Release

#### Trademarks of Infineon Technologies AG

AURIX™, C166™, CanPAK™, CIPOS™, CIPURSE™, CoolMOS™, CoolSET™, CORECONTROL™, CROSSAVE™, DAVE™, DI-POL™, EasyPIM™, EconoBRIDGE™, EconoDUAL™, EconoPIM™, EconoPACK™, EiceDRIVER™, eupec™, FCOS™, HITFET™, HybridPACK™, I<sup>2</sup>RF™, ISOFACE™, IsoPACK™, MIPAQ™, ModSTACK™, my-d™, NovalithIC™, OptiMOS™, ORIGA™, POWERCODE™, PRIMARION™, PrimePACK™, PrimeSTACK™, PRO-SIL™, PROFET™, RASIC™, ReverSave™, SatRIC™, SIEGET™, SINDRION™, SIPMOS™, SmartLEWIS™, SOLID FLASH™, TEMPFET™, thinQ™, TRENCHSTOP™, TriCore™.

#### Other Trademarks

Advance Design System™ (ADS) of Agilent Technologies, AMBA™, ARM™, MULTI-ICE™, KEIL™, PRIMECELL™, REALVIEW™, THUMB™, μVision™ of ARM Limited, UK. AUTOSAR™ is licensed by AUTOSAR development partnership. Bluetooth™ of Bluetooth SIG Inc. CAT-ig™ of DECT Forum. COLOSSUS™, FirstGPS™ of Trimble Navigation Ltd. EMV™ of EMVCo, LLC (Visa Holdings Inc.). EPCOS™ of Epcos AG. FLEXGO™ of Microsoft Corporation. FlexRay™ is licensed by FlexRay Consortium. HYPERTERMINAL™ of Hilgraeve Incorporated. IEC™ of Commission Electrotechnique Internationale. IrDA™ of Infrared Data Association Corporation. ISO™ of INTERNATIONAL ORGANIZATION FOR STANDARDIZATION. MATLAB™ of MathWorks, Inc. MAXIM™ of Maxim Integrated Products, Inc. MICROTREC™, NUCLEUS™ of Mentor Graphics Corporation. MIPI™ of MIPI Alliance, Inc. MIPS™ of MIPS Technologies, Inc., USA. muRata™ of MURATA MANUFACTURING CO., MICROWAVE OFFICE™ (MWO) of Applied Wave Research Inc., OmniVision™ of OmniVision Technologies, Inc. Openwave™ Openwave Systems Inc. RED HAT™ Red Hat, Inc. RFMD™ RF Micro Devices, Inc. SIRIUS™ of Sirius Satellite Radio Inc. SOLARIS™ of Sun Microsystems, Inc. SPANSION™ of Spansion LLC Ltd. Symbian™ of Symbian Software Limited. TAIYO YUDEN™ of Taiyo Yuden Co. TEAKLITE™ of CEVA, Inc. TEKTRONIX™ of Tektronix Inc. TOKO™ of TOKO KABUSHIKI KAISHA TA. UNIX™ of X/Open Company Limited. VERILOG™, PALLADIUM™ of Cadence Design Systems, Inc. VLYNQ™ of Texas Instruments Incorporated. VXWORKS™, WIND RIVER™ of WIND RIVER SYSTEMS, INC. ZETEX™ of Diodes Zetex Limited.

Last Trademarks Update 2011-11-11

[www.infineon.com](http://www.infineon.com)

**Edition 2016-02**

**Published by**

**Infineon Technologies AG**

**81726 Munich, Germany**

**© 2016 Infineon Technologies AG.**

**All Rights Reserved.**

**Do you have a question about any aspect of this document?**

**Email: [erratum@infineon.com](mailto:erratum@infineon.com)**

**Document reference**

**AN\_201509\_PL\_032**

#### Legal Disclaimer

THE INFORMATION GIVEN IN THIS APPLICATION NOTE (INCLUDING BUT NOT LIMITED TO CONTENTS OF REFERENCED WEBSITES) IS GIVEN AS A HINT FOR THE IMPLEMENTATION OF THE INFINEON TECHNOLOGIES COMPONENT ONLY AND SHALL NOT BE REGARDED AS ANY DESCRIPTION OR WARRANTY OF A CERTAIN FUNCTIONALITY, CONDITION OR QUALITY OF THE INFINEON TECHNOLOGIES COMPONENT. THE RECIPIENT OF THIS APPLICATION NOTE MUST VERIFY ANY FUNCTION DESCRIBED HEREIN IN THE REAL APPLICATION. INFINEON TECHNOLOGIES HEREBY DISCLAIMS ANY AND ALL WARRANTIES AND LIABILITIES OF ANY KIND (INCLUDING WITHOUT LIMITATION WARRANTIES OF NON-INFRINGEMENT OF INTELLECTUAL PROPERTY RIGHTS OF ANY THIRD PARTY) WITH RESPECT TO ANY AND ALL INFORMATION GIVEN IN THIS APPLICATION NOTE.

#### Information

For further information on technology, delivery terms and conditions and prices, please contact the nearest Infineon Technologies Office ([www.infineon.com](http://www.infineon.com)).

#### Warnings

Due to technical requirements, components may contain dangerous substances. For information on the types in question, please contact the nearest Infineon Technologies Office. Infineon Technologies components may be used in life-support devices or systems only with the express written approval of Infineon Technologies, if a failure of such components can reasonably be expected to cause the failure of that life-support device or system or to affect the safety or effectiveness of that device or system. Life support devices or systems are intended to be implanted in the human body or to support and/or maintain and sustain and/or protect human life. If they fail, it is reasonable to assume that the health of the user or other persons may be endangered.